1954

Local buckling of wide-flange shapes, Lehigh University, (1954)

G. Haaijer

B. Thurlimann

Welded Continuous Frames and Their Components

Progress Report X

Local Buckling of Wide-Flange Shapes

by

Geerhard Haaijer and Bruno Thürlimann

(Not for Publication)

This work has been carried out as a part of an investigation sponsored jointly by the Welding Research Council and the Department of the Navy with funds furnished by the following:

American Institute of Steel Construction
American Iron and Steel Institute
Institute of Research, Lehigh University
Column Research Council (Advisory)
Office of Naval Research (Contract No.39303)
Bureau of Ships
Bureau of Yards and Docks

Fritz Engineering Laboratory
Department of Civil Engineering & Mechanics
Lehigh University
Bethlehem, Pennsylvania

December, 1954

Fritz Laboratory Report No. 205E.5

TABLE OF CONTENTS

I. Introduction

In order to solve the problem of buckling of a plate, the relationships between additional stress and strains due to the deflection of the plate out of its plane have to be known.

In the elastic range the assumption that the material is isotropic and homogeneous leads to solutions which are in very good agreement with test-results.

Several investigators have given theoretical solutions for buckling in the plastic range based on different stress-strain relationships. The discrepancies between the different theories are basically due to these stress-strain relationships, which by some authors are directly assumed and by others are derived for materials with idealized behavior.

It is the purpose of the local buckling project at Lehigh University to arrive at a solution of this problem which will apply to structural steel plates. Ultimately the aim is to specify the dimensions of rolled shapes in such a way that they can sustain sufficiently large deformations without occurence of local buckling.

In the following theoretical considerations the stress-strain relationships have been kept quite general. Comparison of test results with the solutions obtained in this way will give some indications of the value of the different variables involved.

As long as no other information from direct tests with regard to the stress-strain relationships is available, this seems to be the only way to arrive at a practical solution of

the problem.

II. Stress-Strain Relationships

Consider a plate made out of a material exhibiting a stress-strain curve in simple tension as shown in Figure 1. The notation subsequently used is given in this same figure.

Take the center plane of the plate as the x-y coordinate plane. Compressing the plate in the x-direction into the plastic range up to a stress σ_o may affect all the deformation properties of the material. Hence the tangent moduli E_{tx} and E_{ty} in the x- and y-direction respectively are possibly different. The same may hold for the Poisson's ratios ν_x and ν_y in the x- and y-direction. The shearing modulus G_t may also be affected.

Call

$$\frac{\partial \epsilon_x}{\partial \sigma_x} = \frac{1}{E_{tx}} \qquad \frac{\partial \epsilon_y}{\partial \sigma_y} = \frac{1}{E_{ty}}$$

$$\frac{\partial \epsilon_y}{\partial \sigma_x} = -\frac{\nu_x}{E_{tx}} \qquad \frac{\partial \epsilon_x}{\partial \sigma_y} = -\frac{\nu_y}{E_{ty}} \qquad \ldots \quad (1)$$

$$\frac{\partial \gamma_{xy}}{\partial \tau_{xy}} = \frac{1}{G_t}$$

The assumption is made that no unloading occurs. Then the relationships between the increments of strains as a function of the increments of the stresses can be written as

$$d\epsilon_x = \frac{1}{E_{tx}} d\sigma_x - \frac{\nu_y}{E_{ty}} d\sigma_y$$

$$d\epsilon_y = -\frac{\nu_x}{E_{tx}} d\sigma_x + \frac{1}{E_{ty}} d\sigma_y \qquad \ldots \quad (2)$$

$$d\gamma_{xy} = \frac{1}{G_t} d\tau_{xy}$$

In words these relationships state that, when uniaxially compressed into the plastic range, the originally isotropic material becomes orthogonally anisctropic.

For the case of unloading the material would again behave elastically, but it is now generally agreed, that under test conditions no unloading occurs when a plate starts to buckle.

In the Appendix a short review is given of the derivations and assumptions with regard to the stress-strain relations used in different theories of plate buckling. The results are summarized in Table 1 giving the assumed or derived expressions of E_{tx}, E_{ty}, ν_x, ν_y, and G_t.

Due to the heterogeneous yielding process of steel this material presents an additional problem. A typical stress-strain curve is shown in Figure 2.

As already emphasized in Progress Report T[1] yielding occurs in so-called slip bands and the strain "jumps" from ϵ_y to ϵ_{st}. Therefore, as long as the average strain is in between ϵ_y and ϵ_{st} : the material is nonhomogeneous. Tests have shown that this yielding process is very erratic[1].

For the rotation of a plastic hinge it is in general desirable that the average strain in the flanges of a WF shape reaches the strain hardening range (ϵ average $\geq \epsilon_{st}$). Then the material is again more or less homogeneous and only this case will be considered in the following derivations.

Once a satisfactory solution for the strain-hardening range is obtained, solutions for the intermediate plastic range

($\epsilon_y < \epsilon_{av} < \epsilon_{st}$) can be derived in a way outlined in Progress Report T.(1)

It should be emphasized that for the above presented general incremental stress-strain relationships, E_{tx}, E_{ty}, ν_x, ν_y and G_t possibly depend on the loading path. Theoretically the plate remains plane until buckling occurs. Therefore the loading path would be: σ_x varying from 0 to σ_o with $\sigma_y = \tau_{xy} = 0$. However, due to unavoidable initial imperfections, for the actual loading path: $\sigma_y \neq 0$ and $\tau_{xy} \neq 0$. Direct tests on, for instance, tube specimens under different combinations of loads (tension, internal pressure, torque) could give the answer to this important problem.

III. General Stress-Strain Relations Applied to Buckling of Plates

When a plate is loaded by forces acting in its center plane a state of stress may be reached such that besides the plane position also a bent equilibrium position becomes possible: the plate buckles.

If the transition from the plane to the bent position would occur under constant loads, unloading on the convex side of the plate would be inevitable. However, under test conditions buckling occurs with an increase of load such that no strain reversal takes place.

Shanley proved that the same happens in the case of axially loaded columns. Agreement between his theory applied to rectangular steel columns, which buckled in the strain-hardening range, and test results was shown in Progress Report S(2).

Consider again a plate uniformly compressed in the x-direction up to a stress σ_o causing orthogonal anisotropy. Calling the deflection perpendicular to the center plane w the expressions for the bending and twisting moments become

$$M_x = -\frac{E_{tx} I}{1-\nu_x \nu_y}\left(\frac{\partial^2 w}{\partial x^2} + \nu_y \frac{\partial^2 w}{\partial y^2}\right)$$

$$M_y = -\frac{E_{ty} I}{1-\nu_x \nu_y}\left(\frac{\partial^2 w}{\partial y^2} + \nu_x \frac{\partial^2 w}{\partial x^2}\right) \qquad (3)$$

$$M_{xy} = -2 G_t I \frac{\partial^2 w}{\partial x \partial y}$$

with $I = t^3/12$

t = thickness of plate

The condition that the bent position is an equilibrium position can be expressed by the following differential equation

$$D_x \frac{\partial^4 w}{\partial x^4} + 2H \frac{\partial^4 w}{\partial x^2 \partial y^2} + D_y \frac{\partial^4 w}{\partial y^4} = t\sigma_x \frac{\partial^2 w}{\partial x^2}$$

$$D_x = \frac{E_{tx} I}{1-\nu_x \nu_y} \qquad (4)$$

$$D_y = \frac{E_{ty} I}{1-\nu_x \nu_y}$$

$$2H = \nu_y D_x + \nu_x D_y + 4G_t I$$

The derivation of these equations may be found in the pertinent literature[3]. Only if $H^2 = D_x D_y$, an assumption made by Bleich[4], solutions of this differential equation can be easily obtained.

The condition that both the plane and the bent position are equilibrium positions can also be expressed in terms of work. The additional work done by the external forces due to bending of the plate must equal the change in strain energy of the plate.

This renders the following integral equation

$$\sigma_o t \iint \left(\frac{\partial w}{\partial x}\right)^2 dxdy = \iint \left[D_x \left(\frac{\partial^2 w}{\partial x^2}\right)^2 + D_y \left(\frac{\partial^2 w}{\partial y^2}\right)^2 + \right.$$
$$\left. + \left(\nu_y D_x + \nu_x D_y\right) \left(\frac{\partial^2 w}{\partial x^2}\right)\left(\frac{\partial^2 w}{\partial y^2}\right) + 4 G_t I \left(\frac{\partial^2 w}{\partial x \partial y}\right)^2 \right] dxdy \qquad (5)$$

When external restraints are provided to the plate the right-hand member of equation 5 has to be supplemented by additional terms expressing the work done by these restraints.

By assuming an appropriate deflection surface equation 5 gives an approximate solution. The degree of approximation depends on the correctness of the assumed deflection surface. In any case the result will be on the upper side.

IV. Application of Energy Method to Different Cases of Buckling of Uniformly Compressed Plates

1. Rectangular plate with the loaded edges $x = 0$ and $x = l$ hinged, the unloaded edge $y = 0$ restrained against rotation and the unloaded edge $y = b/2$ free (Figure 3).

In their paper on buckling of outstanding flanges Lundquist and Stowell[5] assumed the following deflection surface, which is known to be good in the elastic range.

$$w = \left[A \frac{2y}{b} + B \left[\left(\frac{2y}{b}\right)^2 + a_1 \left(\frac{2y}{b}\right)^3 + a_2 \left(\frac{2y}{b}\right)^4 + a_3 \left(\frac{2y}{b}\right)^5 \right] \right] \sin \frac{\pi x}{l} . \qquad (6)$$

$$a_1 = -1.0076$$
$$a_2 = +0.5076$$
$$a_3 = -0.1023$$

The ratio B/A depends on the amount of restraint. In the case of elastic restraint with ψ = moment per unit length required for a unit rotation

$$\beta = \frac{B}{A} = \frac{\psi b}{4D_y} \quad . \quad . \quad . \quad . \quad . \quad . \quad . \quad . \quad (7)$$

Substituting w in the energy equation and performing the integrations gives

$$\sigma_o = \frac{t^2}{12(1-\nu_x\nu_y)}\left[E_{tx}\left(\frac{\pi}{l}\right)^2 + E_{ty}\left(\frac{2}{b}\right)^4\left(\frac{l}{\pi}\right)^2 \frac{2\beta+\beta^2 C_3}{1/3+\beta C_1+\beta^2 C_2}\right.$$

$$- (\nu_y E_{tx} + \nu_x E_{ty}) \left(\frac{2}{b}\right)^2 \frac{\beta C_4 + \beta^2 C_5}{1/3+\beta C_1+\beta^2 C_2} \quad . \quad . \quad (8)$$

$$\left. + 4(1-\nu_x\nu_y)G_t\left(\frac{2}{b}\right)^2 \frac{1+\beta C_6+\beta^2 C_7}{1/3+\beta C_1+\beta^2 C_2}\right]$$

with

$$C_1 = 1/2 + 2/5\ a_1 + 1/3\ a_2 + 2/7\ a_3 = 0.23693$$

$$C_2 = 1/5 + 1/3\ a_1 + 1/7\ (a_1^2 + 2a_2) + 1/4\ (a_3 + a_1a_2) + 1/9\ (a_2^2 + 2a_1a_3) + 1/5\ a_2\ a_3 + 1/11\ a_3^2 = 0.04286$$

$$C_3 = 4 + 12\ a_1^2 + 144/5\ a_2^2 + 400/7\ a_3^2 + 12\ a_1 + 16\ a_2 + 20\ a_3 + 36\ a_1a_2 + 48\ a_1a_3 + 80\ a_2a_3 = 0.56712$$

$$C_4 = 1 + 2\ a_1 + 3\ a_2 + 4\ a_3 = 0.0984$$

$$C_5 = 2/3 + 2\ a_1 + 1/5\ (6\ a_1^2 + 14\ a_2) + 1/3\ (11\ a_3 + 9\ a_1a_2) + 1/7\ (26\ a_1a_3 + 12\ a_2^2) + 4\ a_2a_3 + 20/9\ a_3^2 = 0.0216$$

$$C_6 = 2(1 + a_1 + a_2 + a_3) = 0.7954$$

$$C_7 = 4/3 + 3\ a_1 + 1/5\ (9\ a_1^2 + 16\ a_2) + 1/3\ (12\ a_1a_2 + 10\ a_3) + 1/7\ (30\ a_1a_3 + 16\ a_2^2 + 5\ a_2a_3 + 25/9\ a_3 = 0.17564$$

A minimum value of σ_o is obtained for l given by

$$\frac{2l}{b} = \pi\sqrt[4]{\frac{1/3+\beta C_1+\beta^2 C_2}{2\beta+\beta^2 C_3}}\ \sqrt[4]{\frac{E_{tx}}{E_{ty}}} \quad . \quad . \quad . \quad . \quad (9)$$

In the limiting cases when the edge y = 0 is hinged or completely fixed equation (8) reduces to

a. Edge y = 0 is hinged ($\beta = 0$) and $l = L$

$$\sigma_{cr} = \left(\frac{2t}{b}\right)^2 \left[\frac{\pi^2 E_{tx}}{12(1-\nu_x\nu_y)}\left(\frac{b}{2L}\right)^2 + G_t\right] \quad . \quad . \quad . \quad . \quad . \quad (10)$$

For a long plate the first term can be neglected and

$$\sigma_{cr} = \left(\frac{2t}{b}\right)^2 G_t \quad . \quad . \quad . \quad . \quad . \quad . \quad . \quad (11)$$

b. Edge y = 0 is completely fixed ($\beta = \infty$)

The minimum value of σ_o is obtained when the half-wave length l satisfies

$$\frac{2l}{b} = 1.646 \sqrt[4]{\frac{E_{tx}}{E_{ty}}} \quad . \quad . \quad . \quad . \quad . \quad . \quad . \quad (12)$$

Then

$$\sigma_{cr} = \left(\frac{2t}{b}\right)^2 \left[\frac{7.275\sqrt{E_{tx}E_{ty}} - 0.506(\nu_y E_{tx} + \nu_x E_{ty})}{12(1-\nu_x\nu_y)} + 1.371\, G_t\right] \quad (13)$$

2. Rectangular plate with the loaded edges hinged, the unloaded edges having equal restraint against rotation (Figure 4)

For this case the following deflection surface is used[6]

$$w = \left[B\pi\left(\frac{y^2}{d^2} - 1/4\right) + (A+B)\cos\frac{\pi y}{d}\right]\sin\frac{\pi x}{l} \quad . \quad . \quad . \quad . \quad (14)$$

the ratio B/A depending on the amount of restraint. For elastic restraints with ψ = moment per unit length required for a unit rotation

$$\beta = B/A = \frac{\psi d}{2D_y} \quad . \quad . \quad . \quad . \quad . \quad . \quad . \quad . \quad (15)$$

Then

$$\sigma_o = \frac{t^2\pi^2}{12(1-\nu_x\nu_y)}\left[E_{tx}\left(\frac{1}{l}\right)^2 + E_{ty}\frac{L^2}{d^4}\;\frac{1/4 + (C_1 + 2/\pi^2)\beta + \beta^2 C_3}{1/4 + \beta C_1 + \beta^2 C_2} + \right.$$

$$(\nu_y E_{tx} + \nu_x E_{ty})\left(\frac{1}{d}\right)^2\;\frac{1/4 + \beta C_1 + \beta^2 C_4}{1/4 + \beta C_1 + \beta^2 C_2} + \quad . \quad . \quad . \quad (16)$$

$$\left. 4(1-\nu_x\nu_y)G_t\left(\frac{1}{d}\right)^2\;\frac{1/4+\beta C_1 + \beta^2 C_4}{1/4 + \beta C_1 + \beta^2 C_2}\right]$$

with

$$C_1 = 1/2 - 4/\pi^2$$
$$C_2 = \pi^2/60 + 1/4 - 4/\pi^2$$
$$C_3 = 1/4 - 2/\pi^2$$
$$C_4 = 5/12 - 4/\pi^2$$

A minimum value of σ_o is obtained for l given by

$$\frac{l}{d} = \sqrt[4]{\frac{E_{tx}}{E_{ty}}\;\frac{1/4 + \beta C_1 + \beta^2 C_2}{1/4 + (C_1 + 2/\pi^2)\beta + \beta^2 C_3}} \quad . \quad . \quad . \quad . \quad (17)$$

In the limiting cases, when the unloaded edges $y = \pm d/2$ are hinged or completely fixed the minimum values of σ_o are

a. Edges $y = d/2$ are hinged $(\beta = 0)$

$$\sigma_{cr} = \frac{\pi^2}{12}\left(\frac{t}{d}\right)^2\left[\frac{2\sqrt{E_{tx}\,E_{ty}} + \nu_y E_{tx} + \nu_x E_{ty}}{1-\nu_x\nu_y} + 4\,G_t\right] \quad . \quad . \quad (18)$$

with

$$\frac{l}{d} = \sqrt[4]{\frac{E_{tx}}{E_{ty}}} \quad . \quad . \quad . \quad . \quad . \quad . \quad . \quad . \quad (19)$$

b. Edges $y = \pm d/2$ are completely fixed ($\beta = \infty$)

$$\sigma_{cr} = \frac{\pi^2}{12}\left(\frac{t}{d}\right)^2 \left[\frac{4.554\sqrt{E_{tx}E_{ty}} + 1.237\,(\nu_y E_{tx} + \nu_x E_{ty})}{1-\nu_x\nu_y} + 4.943\,G_t \right] \quad . \quad (20)$$

with

$$\frac{l}{d} = 0.66\sqrt{\frac{E_{tx}}{E_{ty}}} \quad . \quad . \quad . \quad . \quad . \quad . \quad . \quad . \quad (21)$$

V. Determination of G_t at the Beginning of Strain-Hardening from Results of Angle Tests

When trying to apply any of the above derived expressions for buckling stresses, the immediate difficulty arises that only the values of E_{tx} and ν_x are known. E_{tx} can be obtained from coupon tests and $\nu_x = 0.5$ for the strain-hardening range (incompressible material). Fortunately, it is possible to obtain a value of G_t from the results of angle tests.

Figures 4 and 5 of Progress Report T[1] show that angle specimens A-31, A-32 and A-33 failed due to torsional buckling at about the point of strain-hardening.

The critical stress for torsional buckling of angles is given by equation (10). Coupon tests gave an average value of E_{tx} at strain-hardening of about $E_{ts} = 900$ ksi.

With assumed values of ν_y, G_{ts} can now be obtained from equation (10)

a. Annealed material (Tests A-31, A-32)

$\sigma_{cr} = 35$ ksi

$\frac{b}{2t} = 8.8$

$\frac{2L}{b} = 2.74$

$\nu_x = \nu_y = 0.5$ $\quad G_{ts} = 2{,}580$ ksi

$\nu_x = 0.5, \nu_y = 1.0$ $\quad G_{ts} = 2{,}510$ ksi

b. As-delivered material (Test A-33)

σ_{cr} = 45 ksi

$\frac{b}{2t}$ = 8.7 $\quad \nu_x = \nu_y = 0.5 \quad G_{ts}$ = 3,270 ksi

$\frac{2l}{b}$ = 2.65 $\quad \nu_x = 0.5, \nu_y = 1.0 \quad G_{ts}$ = 3,210 ksi

From the general expressions summarized in Table I numerical values of E_{tx}, E_{ty}, G_t, ν_x and ν_y are computed for the beginning of the strain-hardening range taking

E_{st} = 900 ksi

E = 30,000 ksi

and ν = 0.3

or ν = 0.5

The results are summarized in Table II. The most important factor for the buckling strength of outstanding flanges is G_t. It is seen that Bleich's semi-rational theory comes closest to the above computed values. However, it may be added that Bleich did not intend to apply his theory to the strain-hardening range of structural steel.

VI. Tests on Wide-Flange Sections

In order to investigate the actual behavior of WF shapes with regard to local buckling 6 shapes were tested under two extreme loading conditions:

(1) Axial compression (Test D1, D2, D3, D4, D5, D6)

(2) Pure bending (Test B1, B2, B3, B4, B5, B6)

The test set-ups for both kinds of tests are shown in Figure 5. The length of each specimen was divided into three gage lengths over which the change in length was measured directly with 0.0001" Ames dials. Along the edges of the flanges and the center of the web, deflection measurements were taken as shown in

the same figure. For the bending tests the lateral rotation was measured at the loading points (which were supported against lateral rotation) and near the center line of the beam. The dimensions of all specimens are given in Table III.

Figure 6 shows the results of tests B1 and D1. First of all P/A vs ϵ_{av} for the compression test and M/Z vs ϵ_{av} for the bending test are plotted

P = compressive load

M = bending moment

A = area of cross-section

Z = plastic section modulus (twice the static moment of half the section about the x-axis)

ϵ_{av} = average strain at center of compressed flange.

Furthermore maximum flange and web deflections are plotted as a function of the average strain and for the bending test the lateral rotation. From these curves the critical strains were obtained and are indicated by arrows. The critical strain is defined as the average strain at which the deflection of flange or web starts to increase more rapidly than it did initially.

The results of the tests on the other sections are presented in the same way in Figures 7 - 11.

Figures 12 - 17 show the strain distribution along the length of the specimens together with flange deflections, web deflections and lateral rotation.

Material properties were obtained from coupon tests, the results of which are given in Table IV.

Figure 18 shows the compression specimens after testing. A side view of the bending specimens is given in Figure 19 and a top view in Figure 20.

VII. Summary of Results

The results of all bending and compression tests are summarized in Table V.

The critical strains of the flanges vs the b/t ratios are plotted in Figure 21. Also the results of the compression tests on angle specimens presented in Progress Report T(1) are included. However, the results of tests D4 and D6 are omitted because web buckling occurred first and obviously caused premature flange buckling. (See Figure 9 and Figure 11).

Furthermore, it is seen from Figure 21 that Stowell's and Bleich's solutions of the problem are conservative. These theoretical solutions are for long hinged flanges corresponding to equation (11). A plot of this equation for the beginning of strain-hardening, for which G_t was found to be $G_{ts} = 2{,}500$ ksi (see chapter V) is given in the same figure.

For the cases where web buckling occurred first, the critical strains are plotted vs the d/w ratio in Figure 22.

From this figure, which also shows plots of equation (18), it can be seen that the value of E_{ty} is probably very close to the value of E (modulus of elasticity).

However, webs of sections are only uniformly compressed in the case of axially loaded columns. For these columns loads rather than deformations are important. Thus critical stresses vs d/w ratios for the webs are plotted in Figure 23.

VIII. Tentative Recommendations for the Geometry of Wide-Flange Shapes

a. Flange Buckling

The requirements for the rotation of a plastic hinge depend on the type of structure and the location of the plastic hinge in the structure.

In Figure 21 all test results are summarized. It is seen that the critical strains increase rapidly near a value $b/t = 17$. For this value the critical strain of a hinged flange just reaches the strain-hardening range.

From a study, which is now being made at Fritz Laboratory on the required rotation capacity of plastic hinges, it is known that in general it is sufficient for the strain of the flanges just to reach the strain-hardening range. Furthermore, it is seen from the test results that in this case no rapid drop of the moment occurs.

Therefore, it can be recommended tentatively to specify $b/t \leq 17$. This will give satisfactory performance of a plastic hinge with respect to local buckling except in special cases of large required rotations producing strains in the flanges far beyond strain-hardening.

b. Web Buckling

For the wide flange shapes subjected to pure bending buckling of the web did not occur for the range of shapes tested:

$$d'/w = 27 \text{ to } 40$$

where

$$d' = d - 2t$$

However, under pure compression web buckling did occur. Taking as the condition that the section can be compressed up to strain-hardening gives

$$\frac{d'}{w} \leqslant 30$$

besides the above specified value of $b/t \leqslant 17$. However, this loading condition only occurs in case of axially loaded columns for which the load rather than the deformation is important. Thus it would be sufficient for the column to reach the yield stress. This happened for test D6 with $d'/w = 39.6$ and $b/t = 18.2$.

Tentatively it can therefore be recommended:

Tentative Specifications		
Compression flanges	for $\epsilon_{cr} = \epsilon_{st}$	b/t = 17
Web subjected to pure bending	to be determined in the future*	
Web subjected to pure compression	for $\epsilon_{cr} = \epsilon_{st}$	d/w = 34
	for $\epsilon_{cr} = \epsilon_{y}$	d/w = 43

*All tested shapes ($d'/w = 27 - 40$) showed satisfactory performance with respect to web buckling and the critical value of d'/w is expected to be considerably higher than 40.

IX. Future Work

A proposal for continuation of the project, 205E, "Inelastic Instability of WF Shapes", was submitted to the Lehigh Project Subcommittee and was approved at its meeting on August 13, 1954. A resume of the program is as follows:

a. Buckling of Web WF-Sections Under Pure Moment

A few tests will be necessary to determine the limiting value of the d/w ratio such that web buckling occurs when the strain of the flanges reaches the strain-hardening range.

c. Buckling of Flanges and Webs Under Moment Gradient

Up till now all bending tests were on WF-sections subjected to pure bending. For the flanges this is probably the most severe loading condition and tests may reveal that under a moment gradient a higher width over thickness ratio could be allowed. In the case of web buckling this loading condition may be more severe than pure bending due to the influence of shear.

d. Stiffening of WF-Sections

If the tests reveal that a large number of available shapes would perform unsatisfactorily, the effect of stiffening devices should be investigated.

e. Lateral Buckling of WF-Beams

The bending tests which were carried out revealed that failure mostly occurred due to a combination of local and lateral buckling. In order to be able to specify the spacing of lateral support more information is needed.

X. Acknowledgements

The authors wish to express their appreciation to Dr. Lynn S. Beedle for his helpful suggestions. The work of Mr. Alfredo T. Gozum on the design of test set-ups and the performance of the tests together with Messrs. Satoru Niimoto and Yuzuru Fujita is gratefully acknowledged. Mr. Fujita also checked the mathematical derivations presented in this report.

The helpful criticisms of members of the Welding Research Council, Lehigh Project Subcommittee (Mr. T. R. Higgins, Chairman) and the Column Research Council Research Committee C (Dr. G. Winter, Chairman) are sincerely appreicated.

Mr. Kenneth R. Harpel, foreman, with his Fritz Laboratory mechanics and technicians prepared the test set-ups and specimens and assisted in every step of the testing program.

This work has been carried out as part of the project, "Welded Continuous Frames and Their Components", being conducted under the general direction of Dr. Lynn S. Beedle.

XI. List of References

1. Thürlimann, B., Haaijer, G., "Buckling of Steel Angles in the Plastic Range", Progress Report T, Fritz Laboratory, Lehigh University, August, 1953.

2. Haaijer, G., "Compression Tests on Short Steel Columns of Rectangular Cross-Section", Progress Report S, Fritz Laboratory, Lehigh University, June, 1953.

3. Girkmann, K., "Flächentragwerke", 2nd Edition, Springer-Verlag, Vienna, 1948, pp. 475-478.

4. Bleich, F., "Buckling Strength of Metal Structures", McGraw-Hill, New York, 1952, pp. 308-310.

5. Lundquist, E.E., Stowell, E.Z., "Critical Compressive Stress for Outstanding Flanges", N.A.C.A., Report 734, 1942.

6. Lundquist, E.E., Stowell, E.Z., "Critical Compressive Stress for Flat Rectangular Plates Supported Along all Edges and Elastically Restrained Against Rotation Along the Unloaded Edges", N.A.C.A. Report No. 733, 1942.

7. Kaufmann, W., "Bemerkungen zur Stabilität Dünnwandiger Kreiszylindrischer Schalen Oberhalb der Proportionalitäts Grenze", Ingenief-Archiv, 1935, Vol. VI No. 6.

8. Bijlaard, P.P., "Some Contributions to the Theory of Elastic and Plastic Stability", Pubs. Intern. Assoc. for Bridge and Structural Engineering, Vol. VIII, 1947.

9. Ilyushin, A.A., "Stability of Plates and Shells Beyond the Proportional Limit", NACA TM-1116, October, 1947.

10. Stowell, E.Z., "A Unified Theory of Plastic Buckling of Columns and Plates", NACA Report 898, 1948.

11. Handleman, G.H., Prager, W., "Plastic Buckling of a Rectangular Plate with Edge Thrust", NACA. TN-1530, 1948.

N O M E N C L A T U R E

A, B, a_1, a_2, a_3, C_1, C_2, C_3, C_4, C_5, C_6, C_7 are constants

A = area of cross-section

E = modulus of elasticity

E_{sec} = secant modulus

E_t = tangent modulus

E_{tx} = tangent modulus in x direction

E_{ty} = tangent modulus in y direction

E_{st} = strain hardening modulus

I = moment of inertia per unit width of plate = $t^3/12$

$$D_x = \frac{E_{tx} I}{1-\nu_x \nu_y}$$

$$D_y = \frac{E_{ty} I}{1-\nu_x \nu_y}$$

$$H = \frac{\nu_y D_x + \nu_x D_y + 4G_t I}{2}$$

G_t = modulus of rigidity

G_{ts} = modulus of rigidity with material compressed to strain hardening

M = bending moment

P = compressive load

Z = plastic section modulus

ϵ_x = strain in x direction

ϵ_y = strain in y direction

ϵ_{av} = average strain at center of compressed flange

ϵ_y = strain at yield point

ϵ_{st} = strain at strain hardening point

γ_{xy} = angular strain in xy plane

σ_x = stress in x direction

σ_y = stress in y direction

σ_o = average compressive stress

σ_y = yield stress

σ_{cr} = critical buckling stress

τ_{xy} = shear stress on xy plane

ν_x = Poisson's ratio for strain in x direction

ν_y = Poisson's ratio for strain in y direction

β = B/A

ψ = edge moment per unit length to produce unit rotation of edge

b/2 = width of plate with one edge free

b = width of flange of WF shape

t = plate thickness

t = thickness of flange of WF shape

d = width of plate supported on both edges

d = depth of WF shape

d' = d-2t

w = thickness of web of WF shape

w = deflection of plate

$\left.\begin{matrix} x \\ y \end{matrix}\right\}$ coordinate axes

l = half wave length of buckled shape

L = length of plate

A P P E N D I X

A review of the stress-strain relationships, used in different theories of plate buckling in the plastic range.

1. Bleich's Theory

Bleich[4] obtains his solution directly from the differential equation (4) taking quite arbitrarily

$$D_x = \frac{E_t I}{1-\nu^2}$$

$$D_y = \frac{EI}{1-\nu^2} \qquad \ldots\ldots\ldots\ldots \quad (22)$$

$$H = \sqrt{D_x D_y}$$

The stress-strain relationships corresponding to the anisotropic behaviour expressed by this differential equation can be derived from equation (22) putting:

$$E_{tx} = E_t \qquad \nu_x = \nu\sqrt{\frac{E_t}{E}}$$

$$E_{ty} = E \qquad \ldots\ldots\ldots\ldots \quad (23)$$

$$G_t = \frac{\sqrt{E\,E_t}}{2(1+\nu)} \qquad \nu_y = \nu\sqrt{\frac{E}{E_t}}$$

Bleich states that this theory must be regarded as a semi-rational theory which can find its justification only by comparison of the theoretical predictions with the results of tests.

2. Kaufmann's Theory

Kaufmann[7] approaches the problem by taking

$$E_{tx} = E_t \,,\; E_{ty} = E \text{ and } \nu_x = \nu_y = \nu \qquad \ldots\ldots\ldots\ldots \quad (24)$$

Using the compatibility and equilibrium conditions for the state of plane stress he derives

$$G_t = \frac{E\,E_t}{(1+\nu)(E+E_t)} \qquad \ldots\ldots\ldots\ldots \quad (25)$$

3. Deformation Theories

The theories of Bijlaard[8], Ilyushin[9] and Stowell[10] are usually referred to as deformation theories.

Their basic assumption is that the relationship between the intensity of stress

$$\sigma_1 = \sqrt{\sigma_x^2 + \sigma_y^2 - \sigma_x\sigma_y + 3\tau_{xy}^2} \quad . \quad . \quad . \quad . \quad . \quad . \quad (26)$$

and the intensity of strain

$$\epsilon_1 = \frac{2}{\sqrt{3}} \sqrt{\epsilon_x^2 + \epsilon_y^2 + \epsilon_x\epsilon_y + \frac{1}{4}\gamma_{xy}^2} \quad . \quad . \quad . \quad . \quad . \quad . \quad (27)$$

is a uniquely defined, single-valued function for any given material if σ_1 increases in magnitude (loading condition)

For a simple coupon test

$$\sigma_1 = \sigma_x$$

and $\epsilon_1 = \epsilon_x$ for Poisson's ratio = 0.5

Therefore,

$$\sigma_1 = E_{sec}\,\epsilon_1 \quad . \quad . \quad . \quad . \quad . \quad . \quad . \quad . \quad (28)$$

E_{sec} = secant modulus (see Figure 1)

The stress-strain relations compatible with equations (26) and (27) are

$$\epsilon_x = \frac{1}{E_{sec}}\left(\sigma_x - \tfrac{1}{2}\sigma_y\right)$$

$$\epsilon_y = \frac{1}{E_{sec}}\left(-\tfrac{1}{2}\sigma_x + \sigma_y\right) \quad . \quad . \quad . \quad . \quad . \quad (29)$$

$$\gamma_{xy} = \frac{3}{E_{sec}}\tau_{xy}$$

The relationships between the increments of stress and strain can be obtained by differentiating equation (29).

The coefficients of these incremental stress-strain relationships will be a function of

For σ_x , σ_y , τ_{xy} , E_{sec} and $E_t = \frac{d\sigma_1}{d\epsilon_1}$

$\sigma_x = \sigma_o$ and $\sigma_y = \tau_{xy} = 0$

one obtains

$$E_{tx} = E_t \qquad \nu_x = 0.5$$

$$E_{ty} = \frac{E_t}{\frac{1}{4} + \frac{3}{4}\frac{E_t}{E_{sec}}} \qquad \nu_y = \frac{1}{\frac{1}{2} + \frac{3}{2}\frac{E_t}{E_{sec}}} \qquad . \quad . \quad . \quad (30)$$

$$G_t = \frac{E_{sec}}{3}$$

4. Flow Theory

Handleman and Prager[11] applied the so-called flow theory to the plate buckling problem. The strain increments are thought to consist of reversible (elastic) and permanent (plastic) components

$$\begin{aligned} d\epsilon_x &= d\epsilon_x' + d\epsilon_x'' \\ d\epsilon_y &= d\epsilon_y' + d\epsilon_y'' \\ d\epsilon_z &= d\epsilon_z' + d\epsilon_z'' \\ d\gamma_{xy} &= d\gamma_{xy}' + d\gamma_{xy}'' \end{aligned} \qquad . \quad . \quad . \quad . \quad . \quad . \quad . \quad (31)$$

For the elastic components Hook's law holds

$$\begin{aligned} E\, d\epsilon_x' &= d\sigma_x - \nu d\sigma_y \\ E\, d\epsilon_y' &= -\nu\sigma d_x + d\sigma_y \\ E\, d\epsilon_z' &= -\nu d\sigma_x - \nu d\sigma_y \\ \frac{E}{2(1+\nu)}\, d\gamma_{xy} &= d\tau_{xy} \end{aligned} \qquad . \quad . \quad . \quad . \quad . \quad . \quad (32)$$

and for the plastic components

$$
\begin{aligned}
E\, d\epsilon_x'' &= a' d\sigma_x + b' d\sigma_y \\
E\, d\epsilon_y'' &= a'' d\sigma_x + b'' d\sigma_y \\
E\, d\epsilon_z'' &= a''' d\sigma_x + b''' d\sigma_y \\
E\, d\gamma_{xy}'' &= 2c' d\tau_{xy}
\end{aligned}
\qquad \ldots \qquad (33)
$$

The coefficients a', a'', a''', b', b'', b''' and c' depend on the existing stress σ_o

It is possible to determine a', a'' and a''' considering that:

1. Plastic deformations do not cause any change in volume

$$d\epsilon_x'' + d\epsilon_y'' + d\epsilon_z'' = 0 \qquad \ldots \qquad (34)$$

2. The y- and z-axis are symmetric with respect to the direction of compression x

$$a'' = a''' \qquad \ldots \qquad (35)$$

3. For a simple coupon test

$$d\sigma_x = E_t\, d\epsilon_x \qquad \ldots \qquad (36)$$

The result is $a' = -2a'' = -2a''' = \frac{E}{E_t} - 1$ (37)

Next the criterion for neutral changes of stresses is considered. It is assumed that

4. The criterion for loading or unloading is furnished by the sign of the work dW which the existing stresses do on the change of shape produced by the increments of stress.

5. The total strain increments will be continuous in the region which marks the transition from unloading through the neutral state to loading. (For neutral changes of stress no plastic deformations occur).

This furnishes the conditions

$$\begin{aligned} a' + 2b' &= 0 \\ a'' + 2b'' &= 0 \\ a''' + 2b''' &= 0 \\ c' &= 0 \end{aligned} \qquad . \quad . \quad . \quad . \quad . \quad . \quad . \quad . \quad (38)$$

Combining equations 32 and 33 finally gives

$$E_{tx} = E_t \qquad \nu_x = \frac{E_t(2\nu - 1) + E}{2E}$$

$$E_{ty} = \frac{4EE_t}{E + 3E_t} \qquad \nu_y = \frac{2\left[E_t(2\nu - 1) + E\right]}{E + 3E_t} \quad . \quad . \quad (39)$$

$$G_t = \frac{E}{2(1+\nu)}$$

TABLE I

Theory	E_{tx}	E_{ty}	G_t	ν_x	ν_y
Bleich (4)	E_t	E	$\frac{\sqrt{E\,E_t}}{2(1+\nu)}$	$\nu\sqrt{\frac{E_t}{E}}$	$\nu\sqrt{\frac{E}{E_t}}$
Kaufmann (7)	E_t	E	$\frac{E\,E_t}{(1+\nu)(E+E_t)}$	ν	ν
Bijlaard (8) Ilyushin (9) Stowell (10)	E_t	$\frac{E_t}{\frac{1}{4}+\frac{3}{4}\frac{E_t}{E_{sec}}}$	$\frac{E_{sec}}{3}$	$\frac{1}{2}$	$\frac{1}{\frac{1}{2}+\frac{3}{2}\frac{E_t}{E_{sec}}}$
Handelmann (11) Prager (11)	E_t	$\frac{4EE_t}{E+3E_t}$	$\frac{E}{2(1+\nu)}$	$\frac{E_t(2\nu-1)+E}{2E}$	$\frac{2[E_t(2\nu-1)+E]}{E+3E_t}$

TABLE II

Theory		E_{tx} ksi	E_{ty} ksi	G_t ksi	ν_x	ν_y
Bleich	$\nu = 0.5$	900	30,000	1,730	0.09	2.39
	$\nu = 0.3$	900	30,000	2,000	0.05	1.73
Kaufmann	$\nu = 0.5$	900	30,000	580	0.5	0.5
	$\nu = 0.3$	900	30,000	670	0.3	0.3
Bijlaard Ilyushin	$\sigma_y = 35$ ksi $\epsilon_s = 13 \times 10^{-3}$	900	1,760	860	0.5	0.98
Stowell	$\sigma_y = 45$ ksi $\epsilon_s = 13 \times 10^{-3}$	900	2,000	1,110	0.5	1.10
Handelman Prager	$\nu = 0.3$	900	3,300	11,500	0.49	1.82

TABLE III

Dimensions of Specimens

Spec.	Shape	A in^2	Z in^3	b in	t in	d in	w in	L in	L^1 in	C in	b/t	d'/w	d/w
B1 D1	10 WF 33	9.66	38.56	7.95	0.429	9.80	0.294	32	32	38	18.5	30.4	33.3
B2 D2	8 WF 24	6.83	22.56	6.55	0.383	8.01	0.236	26	26	38	17.1	30.7	33.9
B3 D3	10 WF 39	11.34	45.63	8.02	0.512	9.88	0.328	32	32	48	15.6	27.0	30.1
B4 D4	12 WF 50	14.25	70.28	8.18	0.620	12.19	0.351	32	32	52	13.2	31.2	34.7
B5 D5	8 WF 35	10.00	33.68	8.08	0.476	8.13	0.308	32	32	44	17.0	23.3	26.4
B6 D6	10 WF 21	5.84	22.45	5.77	0.318	9.82	0.232	23	26	30	18.2	39.6	42.3

$d' = d - 2t$

TABLE IV

Results of Coupon Tests

Coupon	Section	Buckling Tests	*Location	Yield Stress σ_y ksi	Strain at Strain-Hardening $\epsilon_{st} \times 10^3$	Strain-Hardening Modulus E_{st} ksi	Type of Loading
T 6	10 WF 33	B1-D1	1	35.5	16.5	675	tension
T 7			5	35.0	14.7	750	tension
C 14			2	40.0	14.5	855	compression
C 15			6	37.0	13.8	805	compression
T 21	8 WF 24	B2-D2	1	35.4	18.4	530	tension
T 22			2	35.6	18.0	600	tension
T 23			3	36.3	19.3	470	tension
T 31	10 WF 39	B3-D3	1	35.6	14.3	525	tension
T 32			2	36.8	18.9	580	tension
T 33			3	37.8	16.3	580	tension
T 41	12 WF 53	B4-D4	1	37.1	18.0	500	tension
T 42			2	36.9	18.1	530	tension
T 43			3	39.4	15.9	580	tension
T 51	8 WF 35	B4-D5	1	37.6	16.9	560	tension
T 52			2	37.3	16.6	465	tension
T 53			3	39.9	19.6	600	tension
T 61	10 WF 21	B6-D6	1	38.0	20.8	520	tension
T 62			2	34.2	23.4	570	tension
T 63			3	44.2	23.6	490	tension

*See Figure

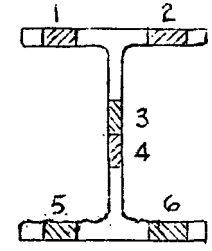

Location of Coupons

All coupons tested in Baldwin 60,000# Hydraulic Machine.
Valve opening corresponding to testing speed of 1 micro-in./in. per sec. in the elastic range.

TABLE V

Test Results

Test	σ_y ksi	$\epsilon_{cr} \cdot 10^3$		σ_{cr} ksi	
		Flange	Web	Flange	Web
D 1	34.4	8.5	8.5	34.2	34.2
D 2	34.0	13.5	12.7	34.0	34.0
D 3	35.2	19.0	19.0	39.0	39.0
D 4	35.0	18.5	5.0	36.8	35.4
D 5	36.6	17.0	17.0	38.0	38.0
D 6	38.0	4.3	1.6	33.8	37.2
B 1		7.0			
B 2		23.0			
B 3		22.5			
B 4		29.0			
B 5		22.0			
B 6		14.0			

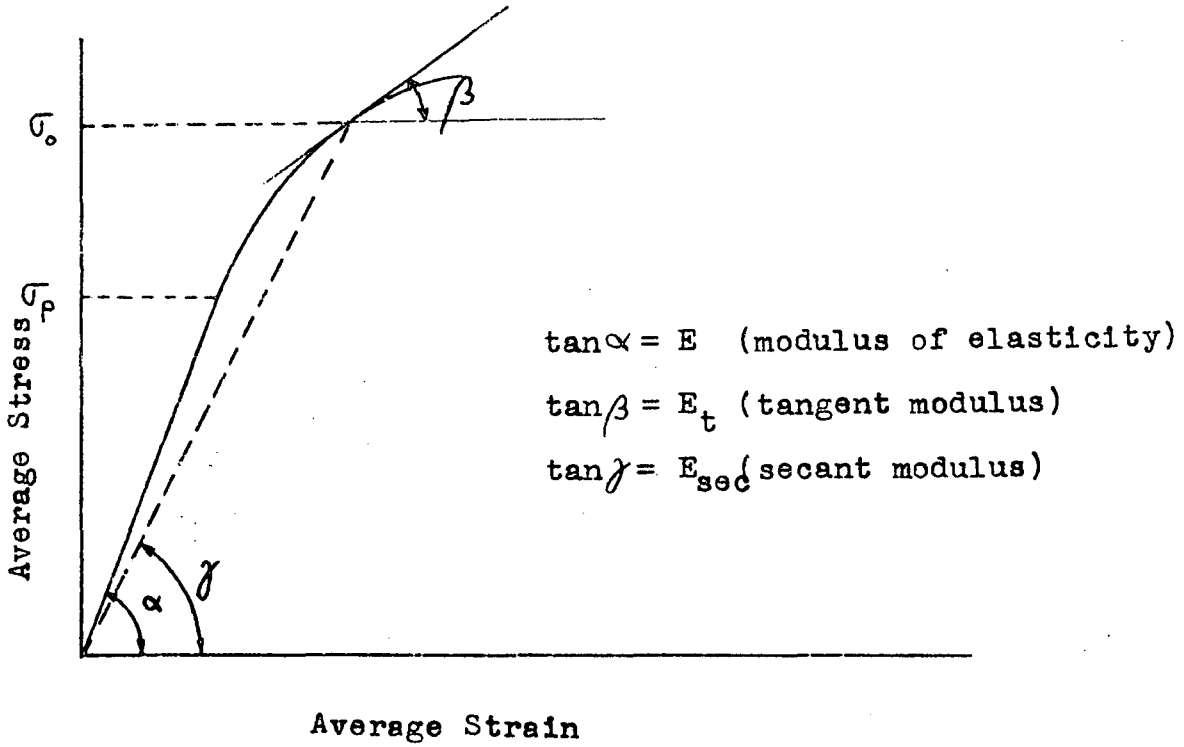
σ_o
σ_p
Average Stress
β
α
γ
$\tan\alpha = E$ (modulus of elasticity)
$\tan\beta = E_t$ (tangent modulus)
$\tan\gamma = E_{sec}$ (secant modulus)
Average Strain

Fig. 1

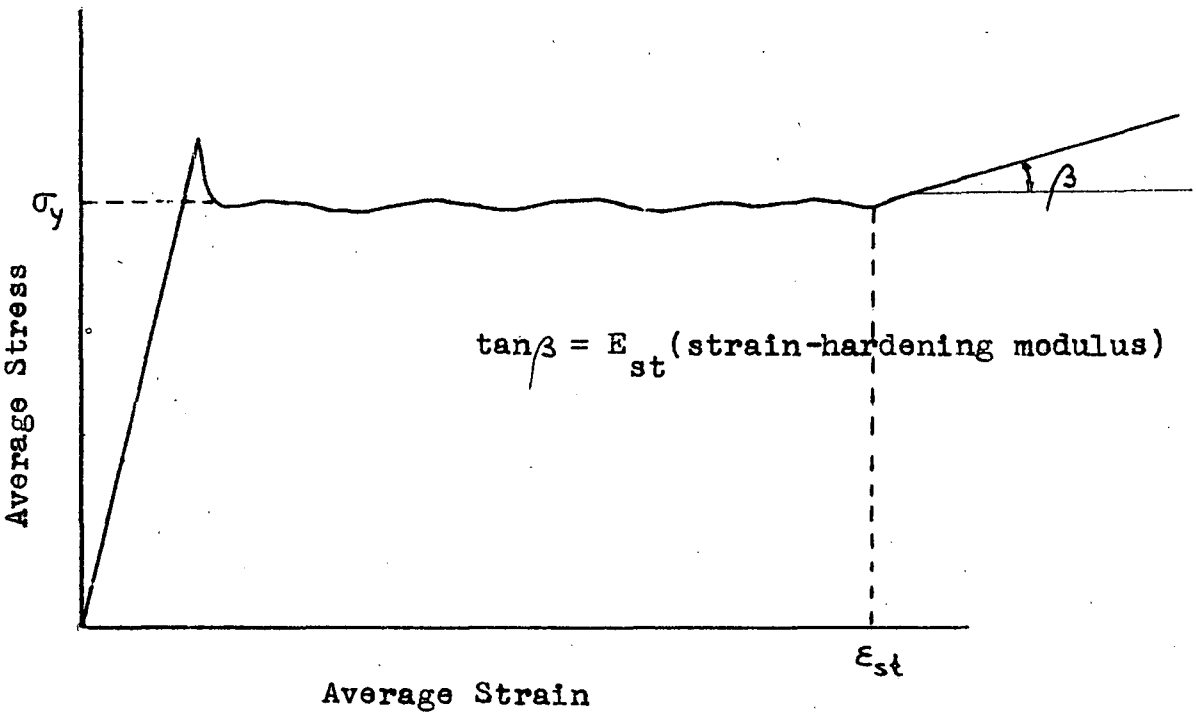
σ_y
Average Stress
β
$\tan\beta = E_{st}$ (strain-hardening modulus)
ε_{st}
Average Strain

Fig. 2

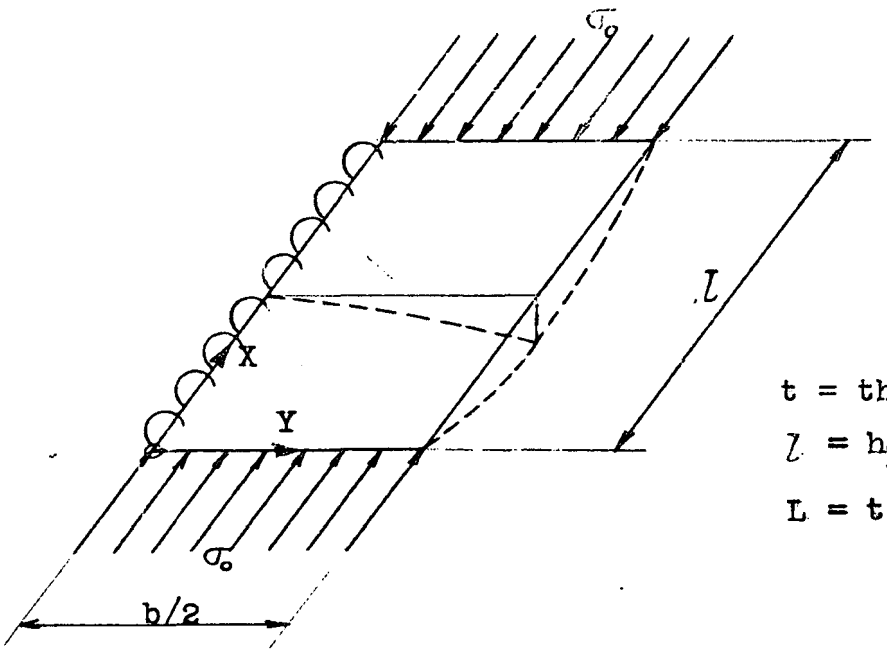

t = thickness of plate

l = half wave length of buckled shape.

L = total length of plate

Fig. 3

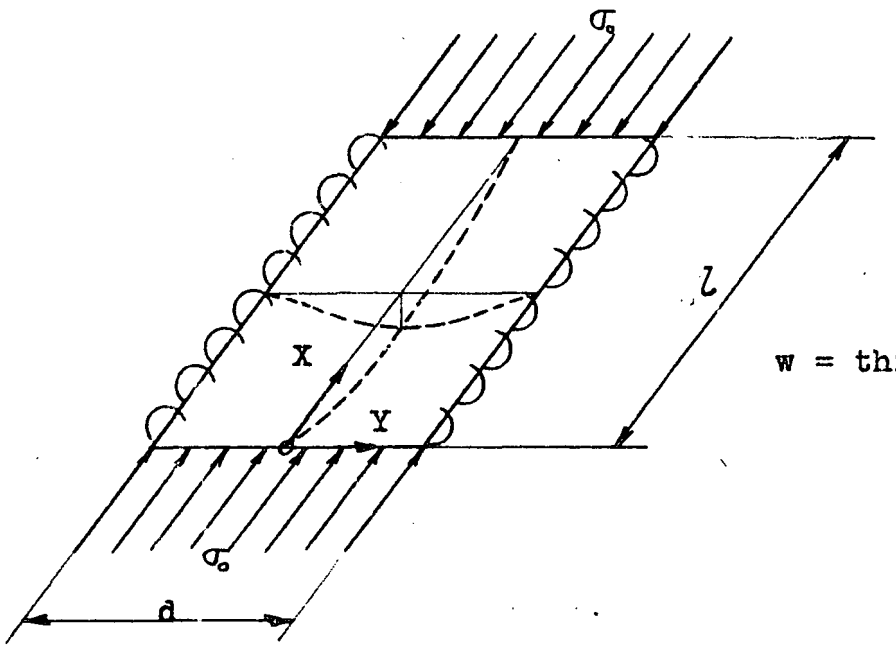

w = thickness of plate

Fig. 4

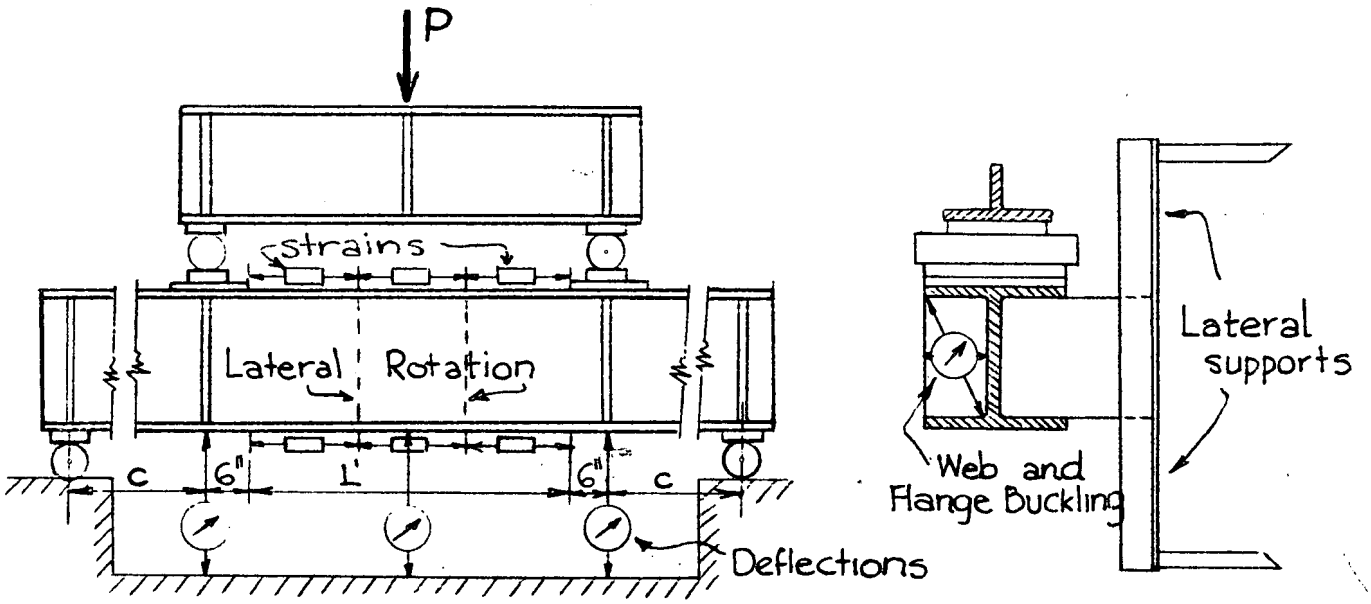

BENDING TEST — B SPECIMENS

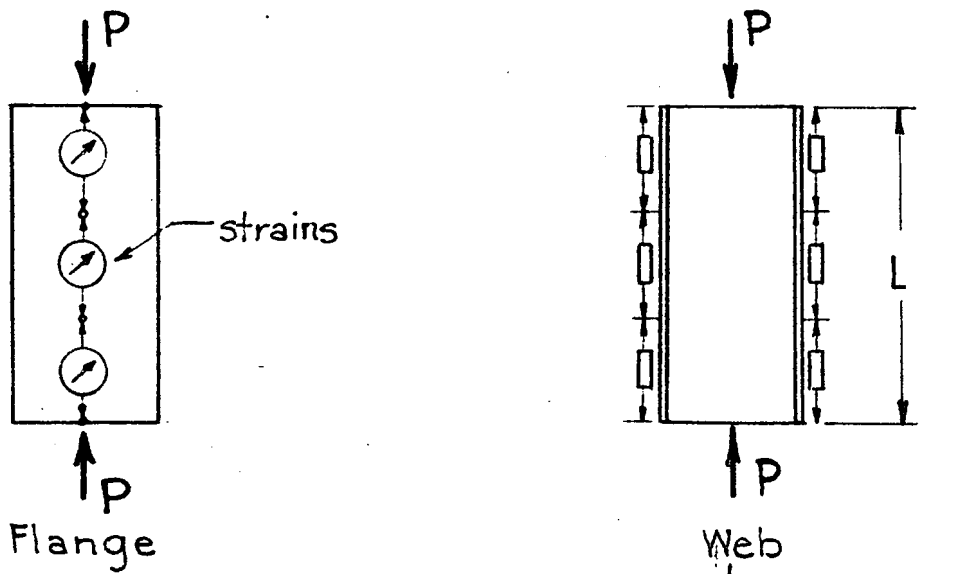

COMPRESSION TEST — D SPECIMENS

Figure 5. Test Set-ups.

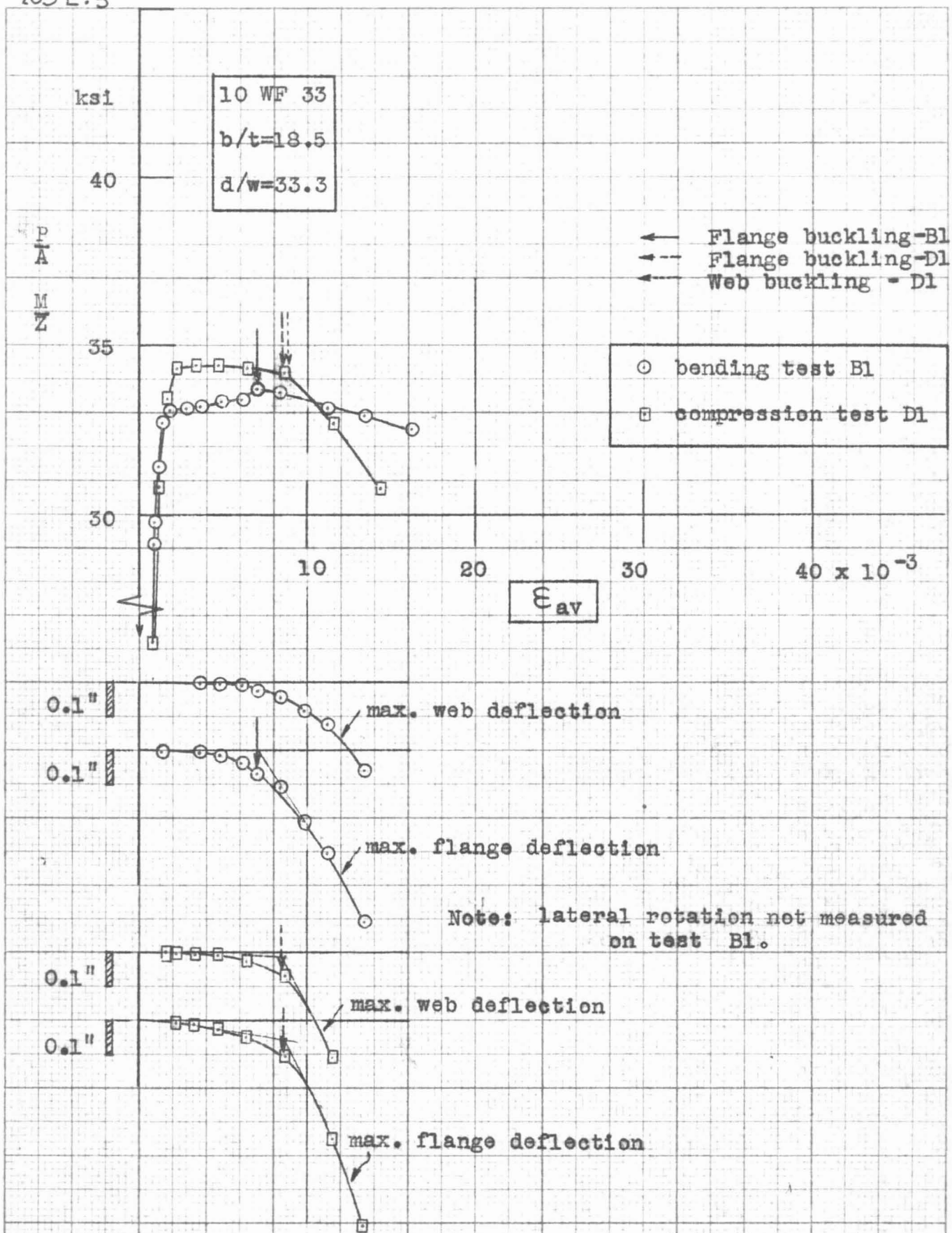

Figure 6. Test Results B1 - D1.

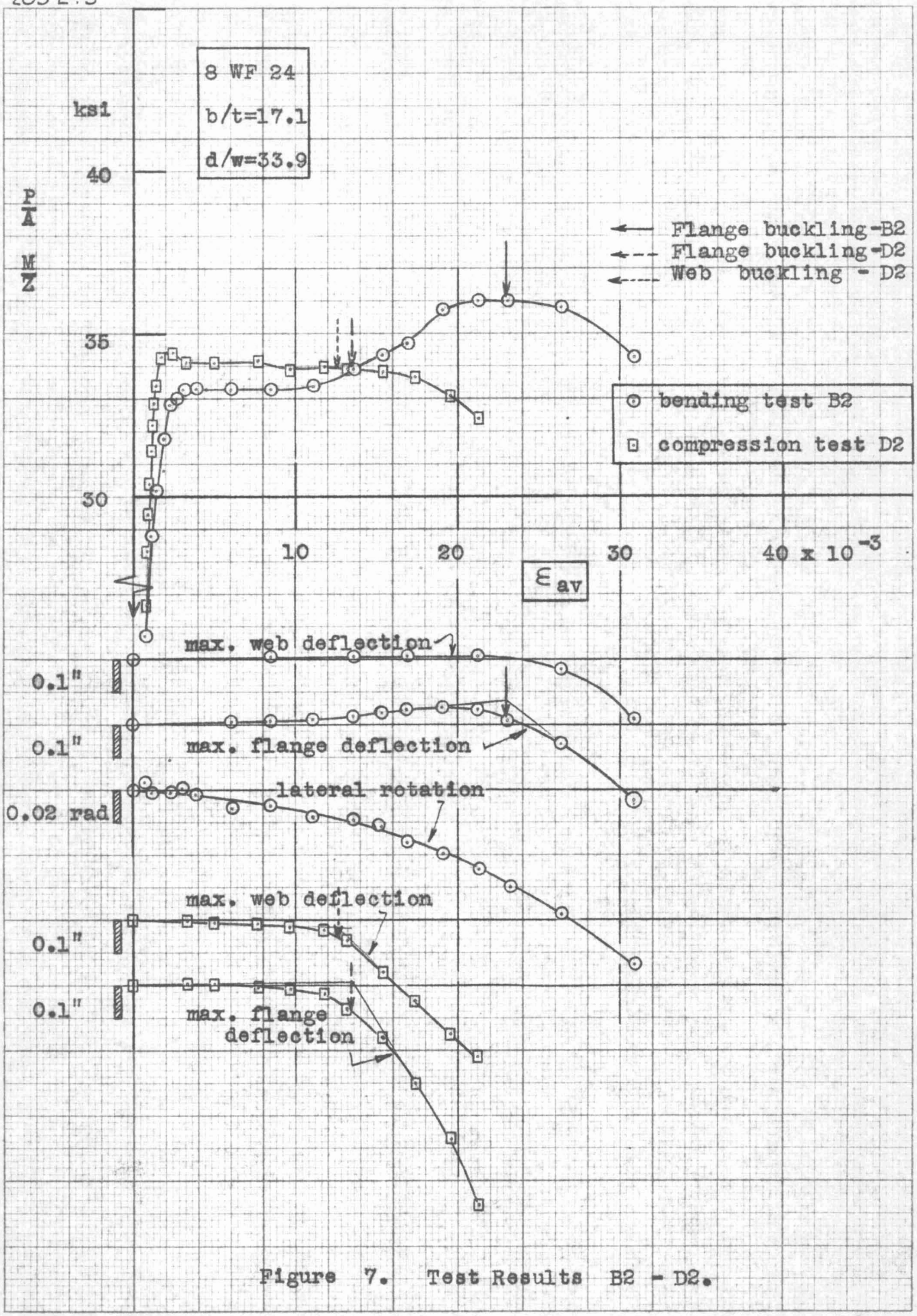

Figure 7. Test Results B2 - D2.

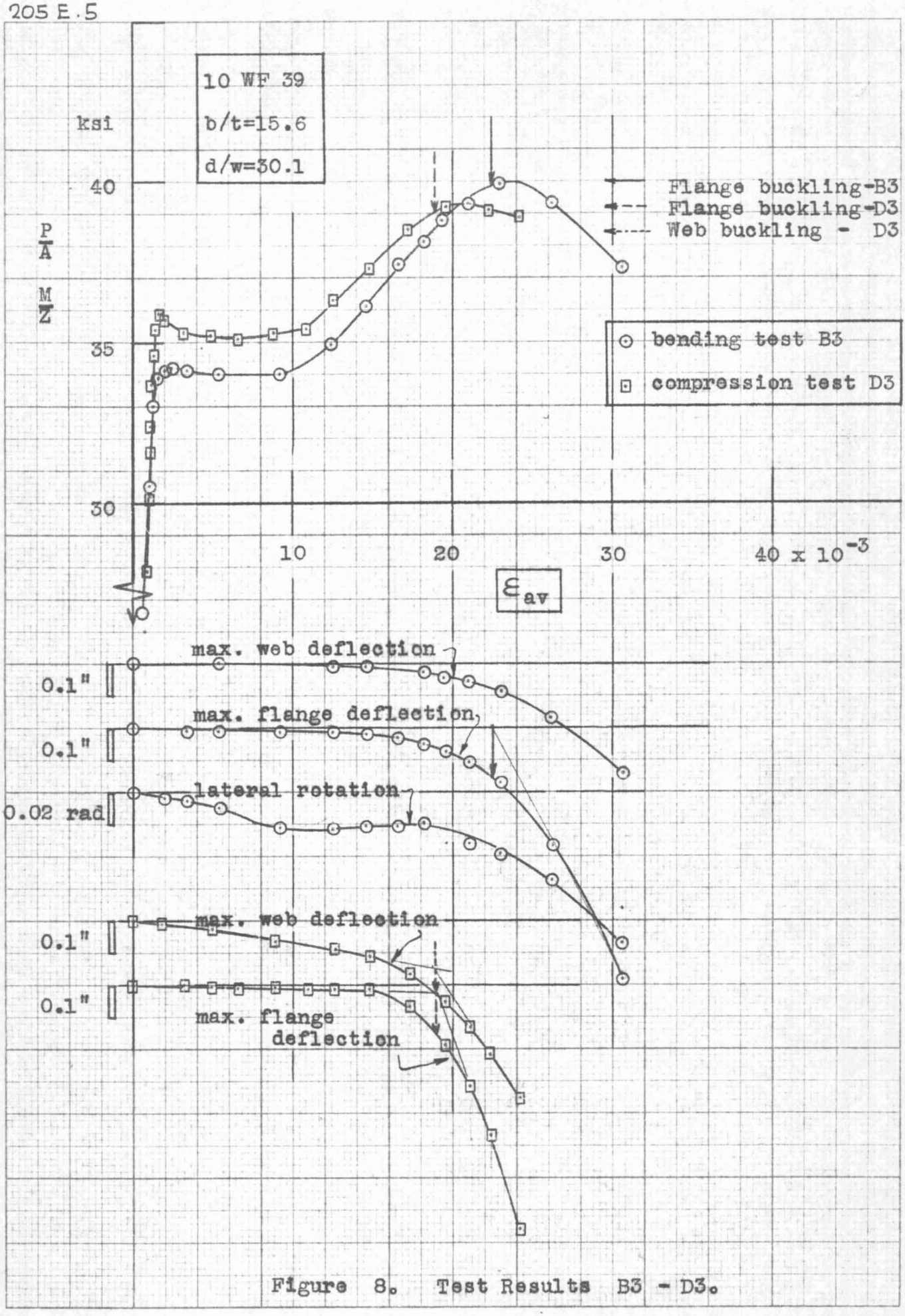

Figure 8. Test Results B3 - D3.

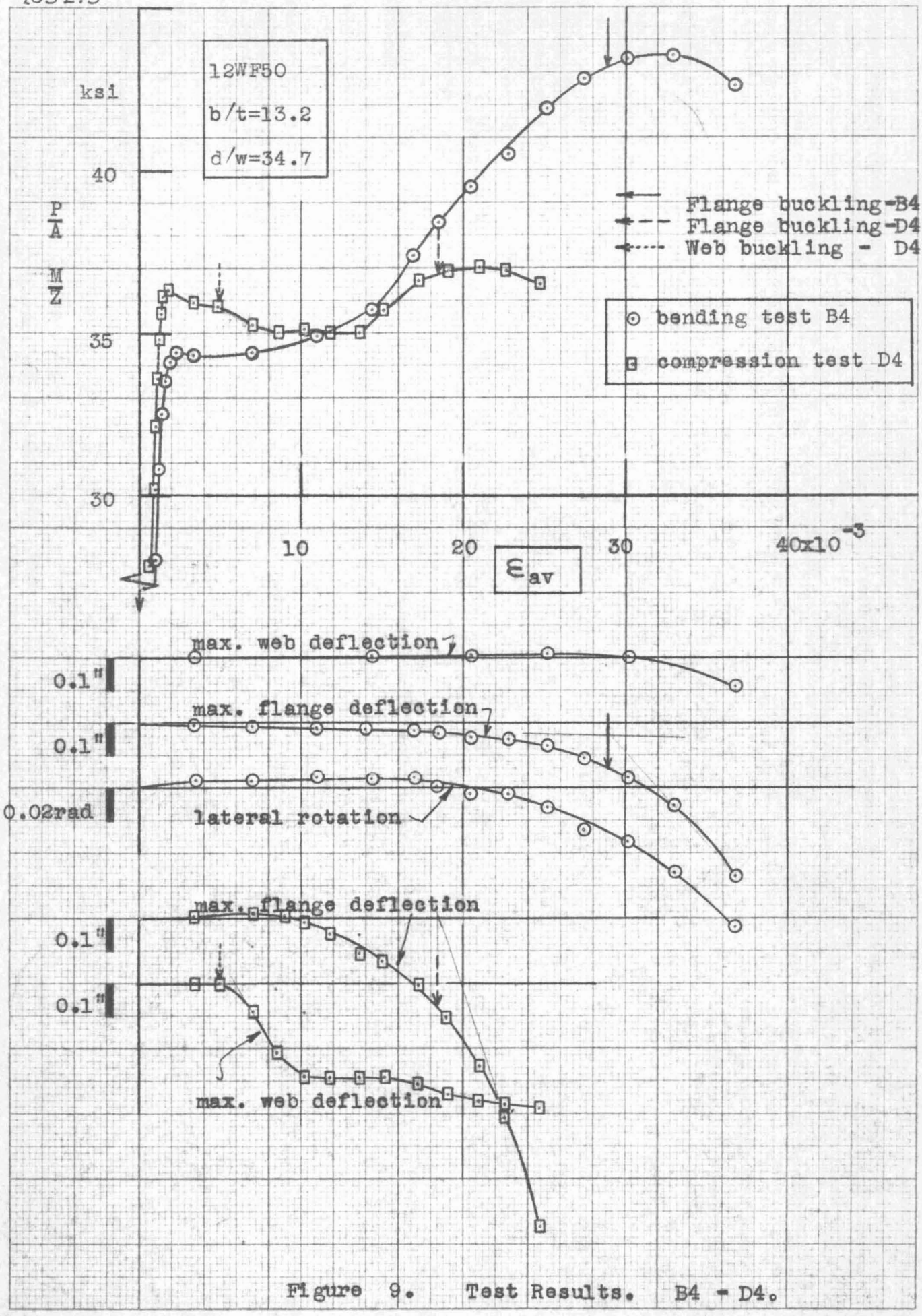

Figure 9. Test Results. B4 - D4.

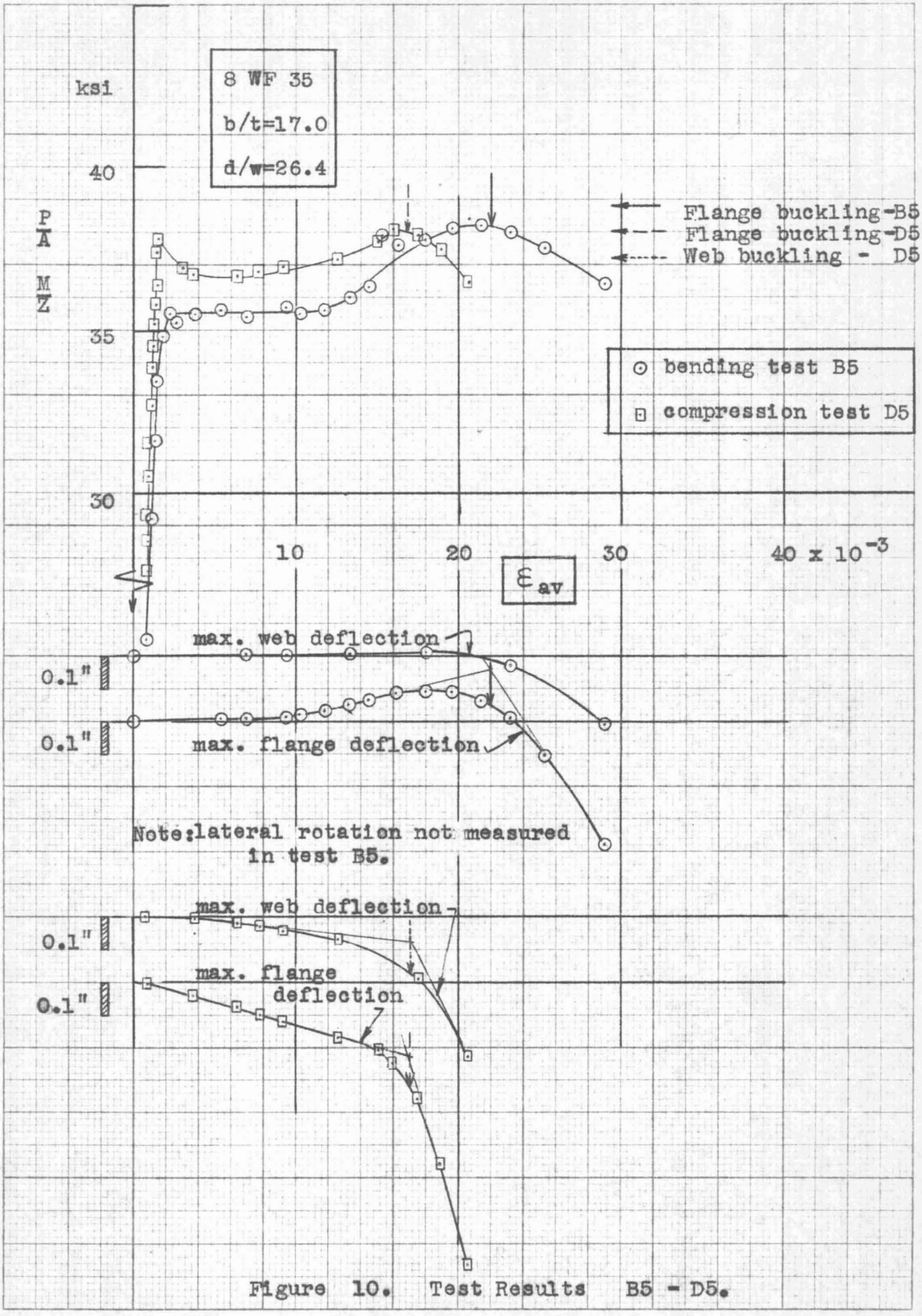

Figure 10. Test Results B5 - D5.

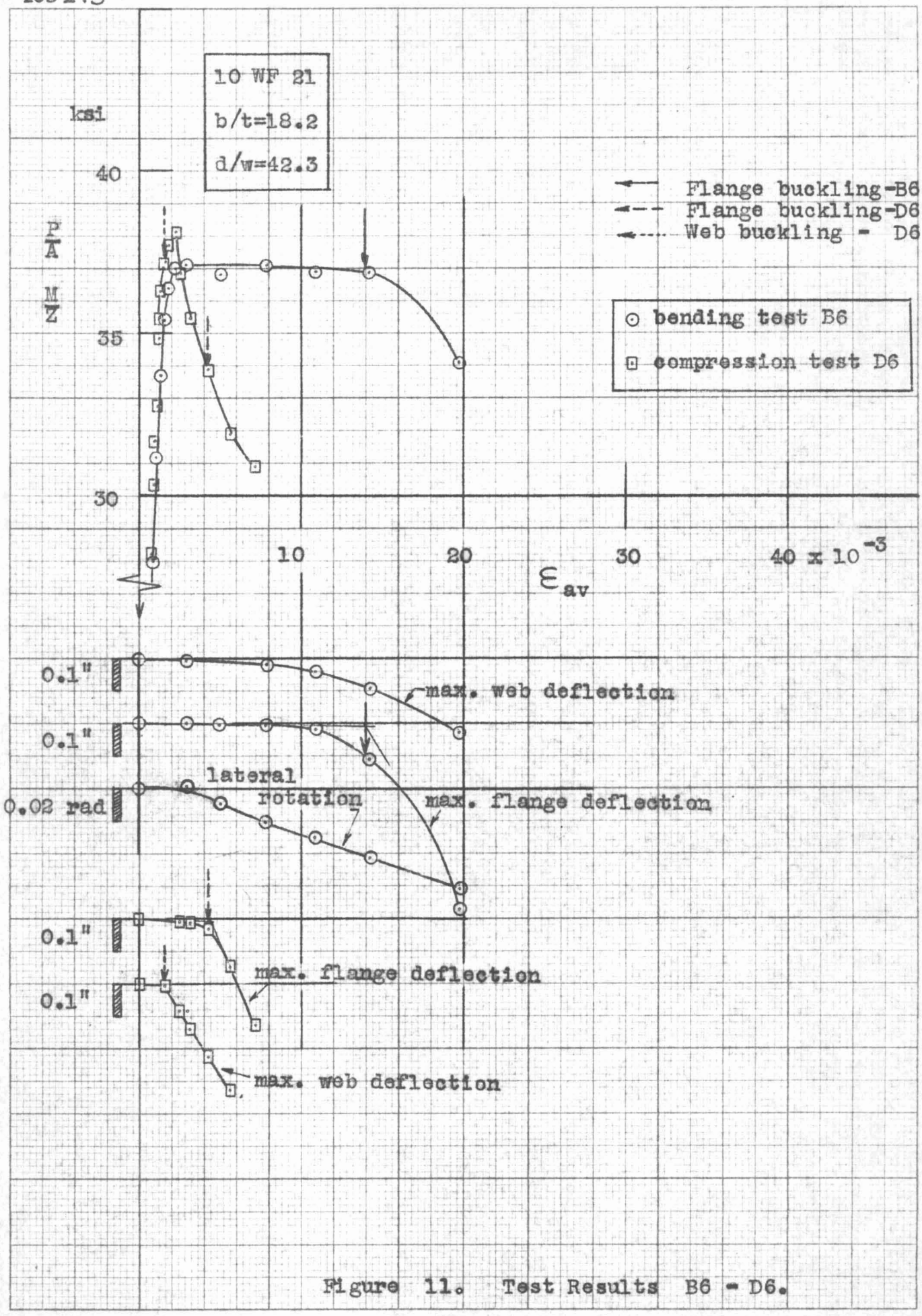

Figure 11. Test Results B6 - D6.

Lateral Rotation not measured

East Loading Point

West Loading Point

Deflection of N. Flange

Average strain calculated from curvature

BENDING TEST B1

⊖——⊖ at $\varepsilon_{av.} = 7.05 \times 10^{-3}$

⊖- - - -⊖ at $\varepsilon_{av.} = 13.39 \times 10^{-3}$

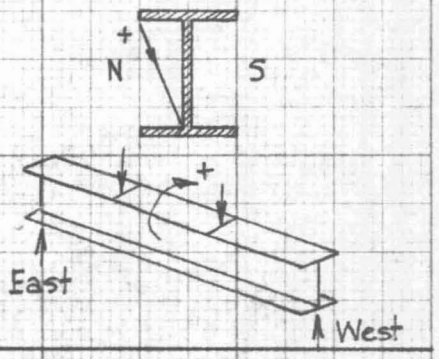

Average strain only measured.

20×10^{-3}

10

0

Strain - N. Flange

Deflections - N. Flange

Deflections - Web

Deflections - S. Flange

20×10^{-3}

10

0

Strain - S. Flange

COMPRESSION TEST D1

□——□ at $\varepsilon_{av.} = 8.66 \times 10^{-3}$

□- - - -□ at $\varepsilon_{av.} = 11.50 \times 10^{-3}$

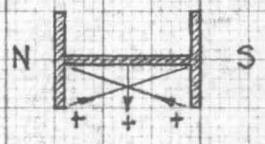

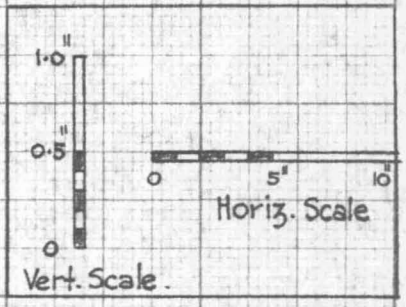

Figure 12. Flange and Web Buckling. B1 - D1

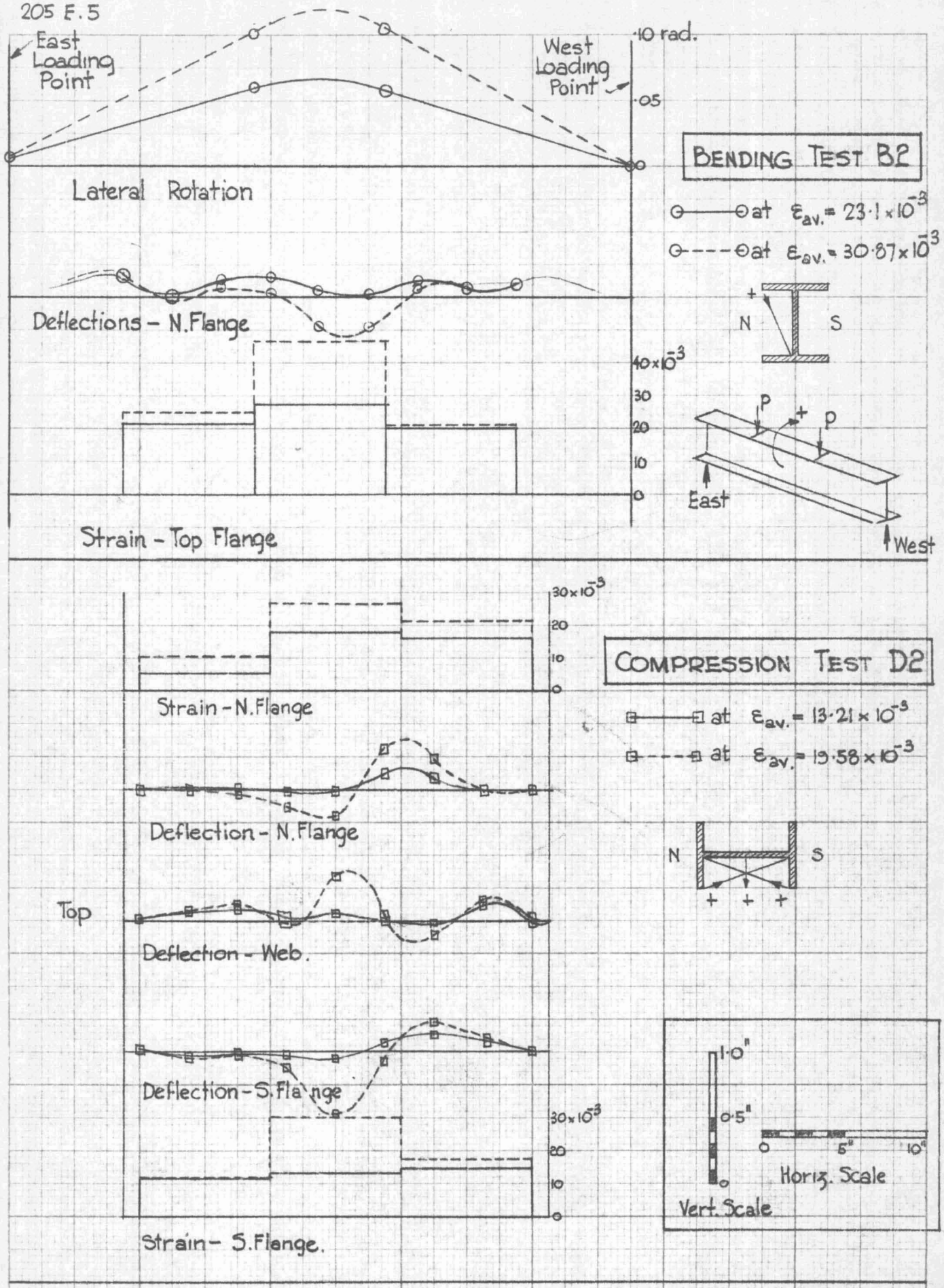

Figure 13. Flange and Web Buckling. B2 - D2.

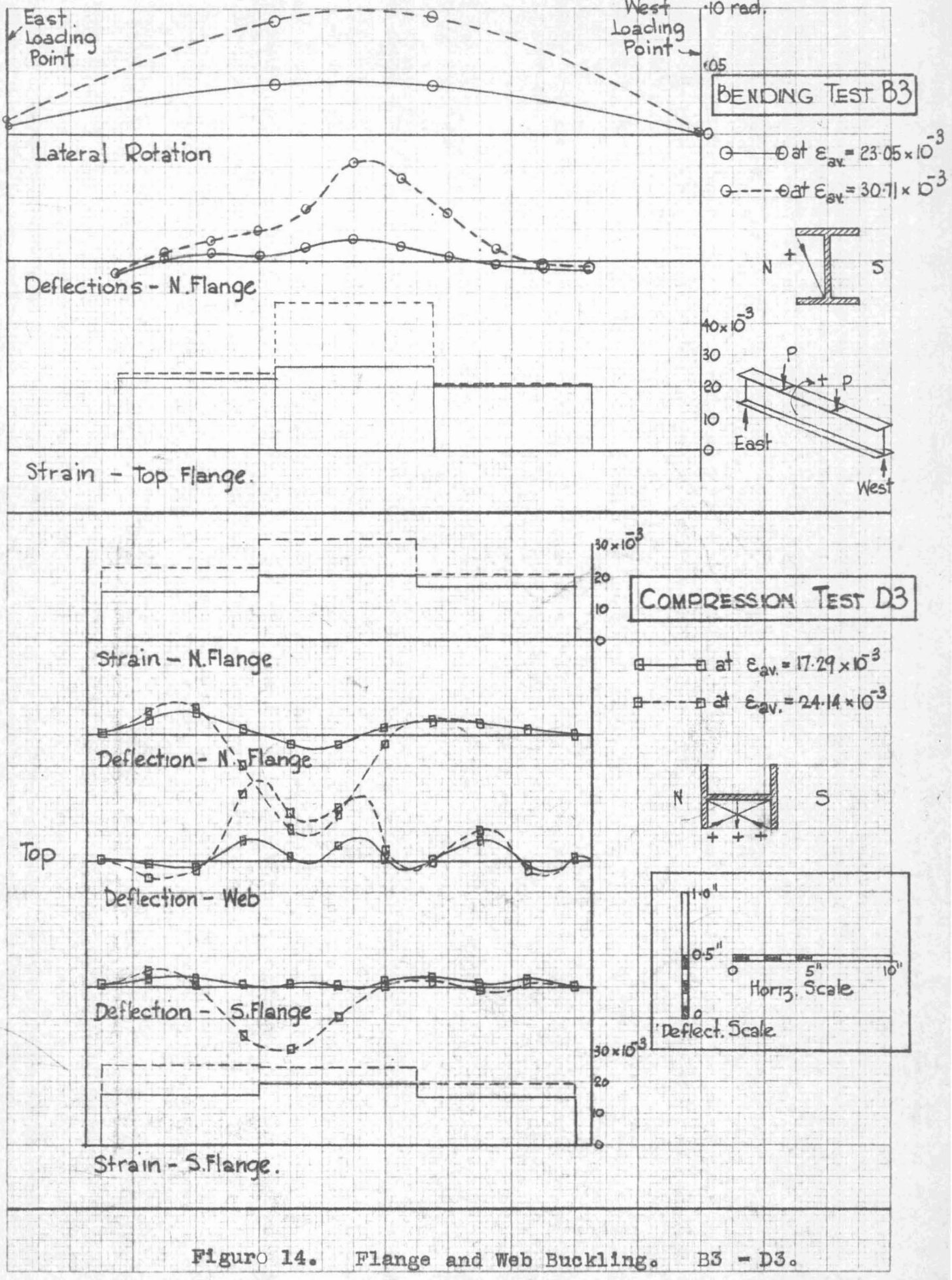

Figure 14. Flange and Web Buckling. B3 - D3.

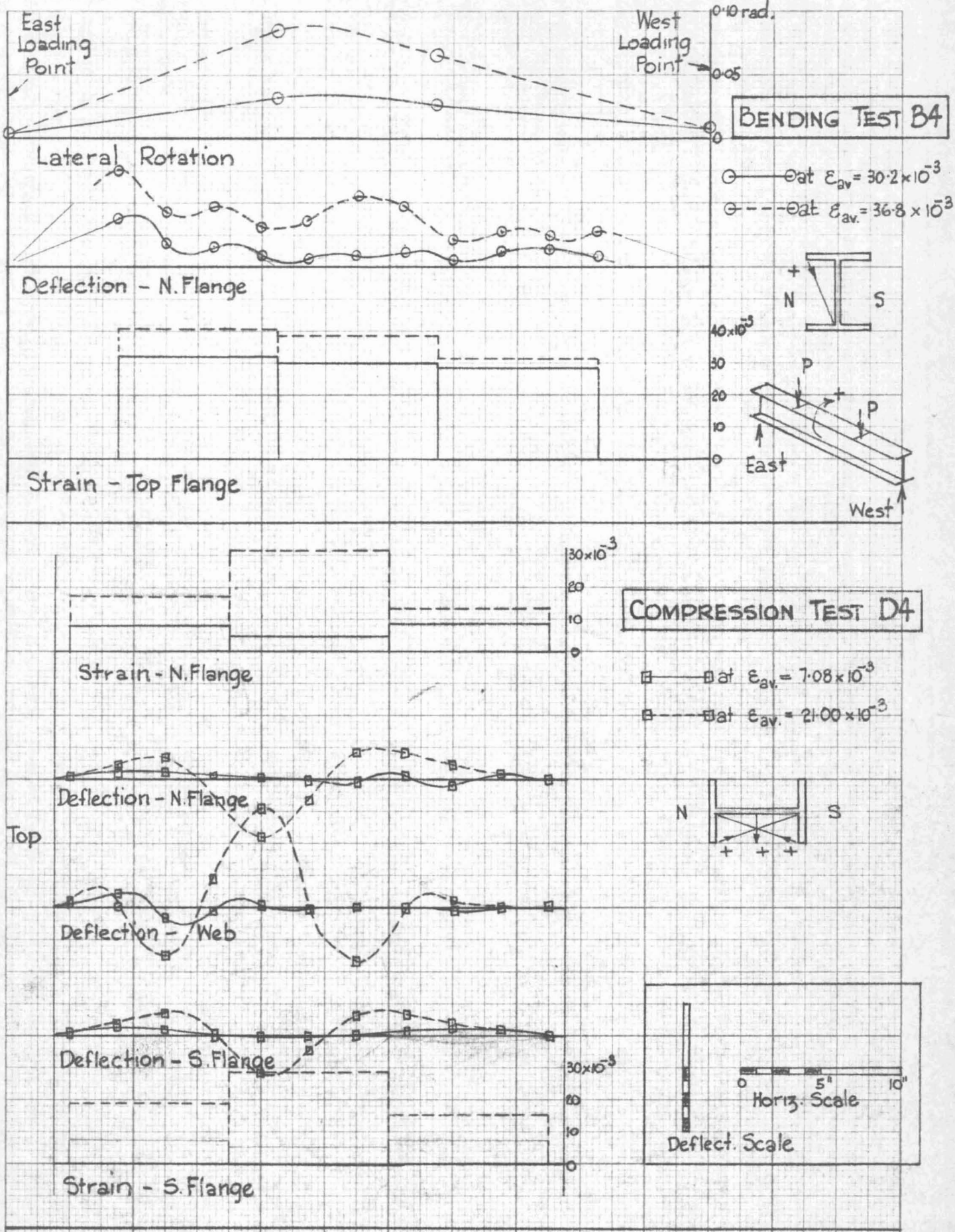

Figure 15. Flange and Web Buckling. B4 - D4.

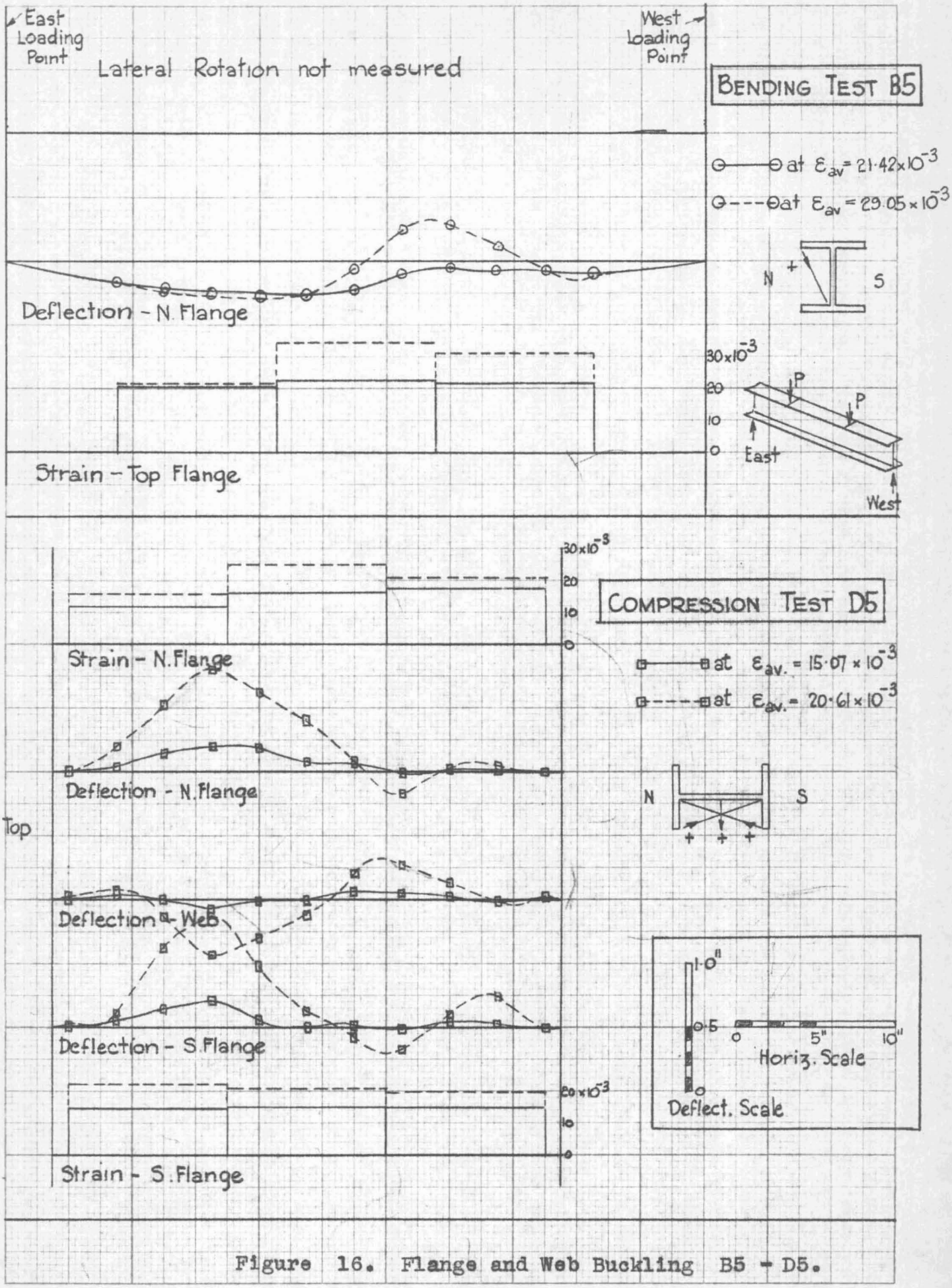

Figure 16. Flange and Web Buckling B5 - D5.

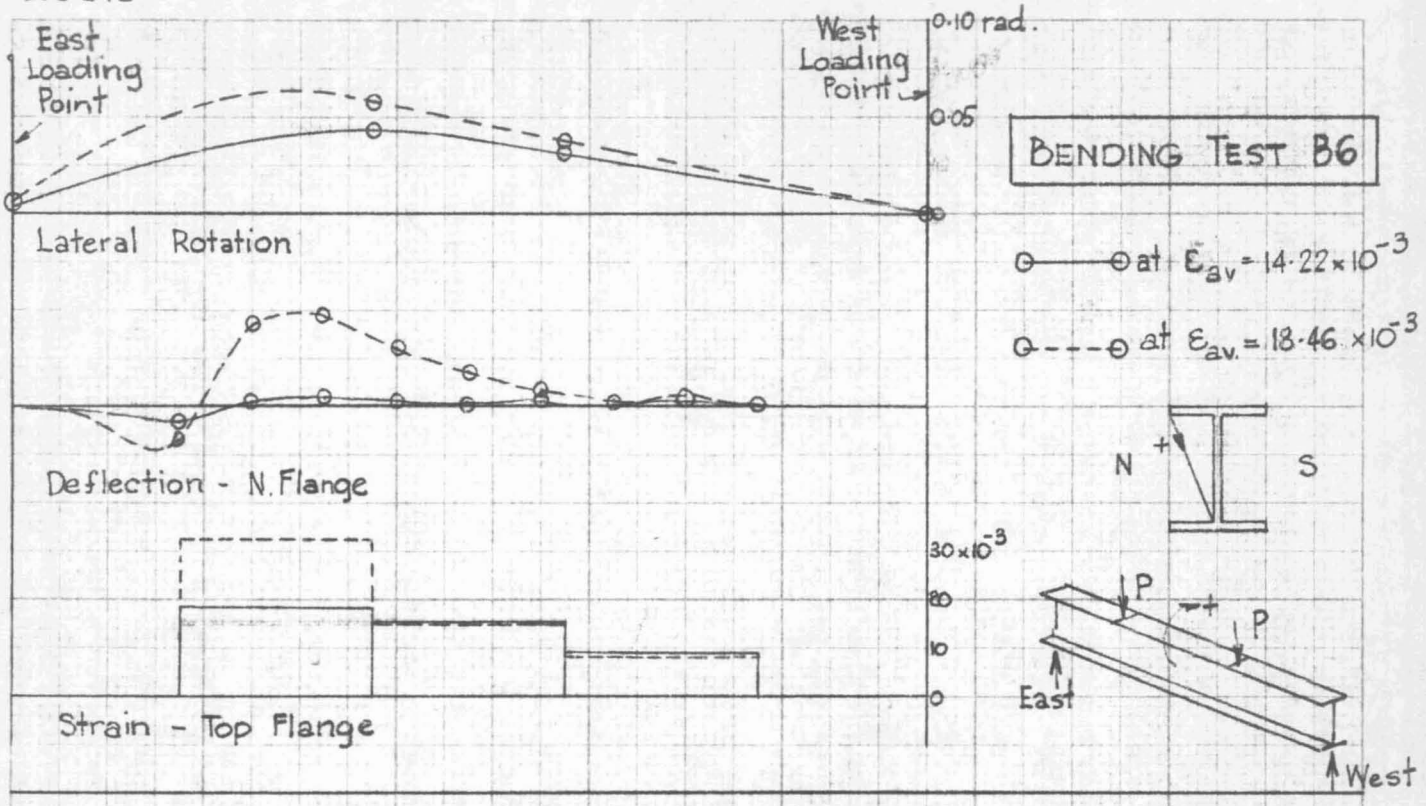

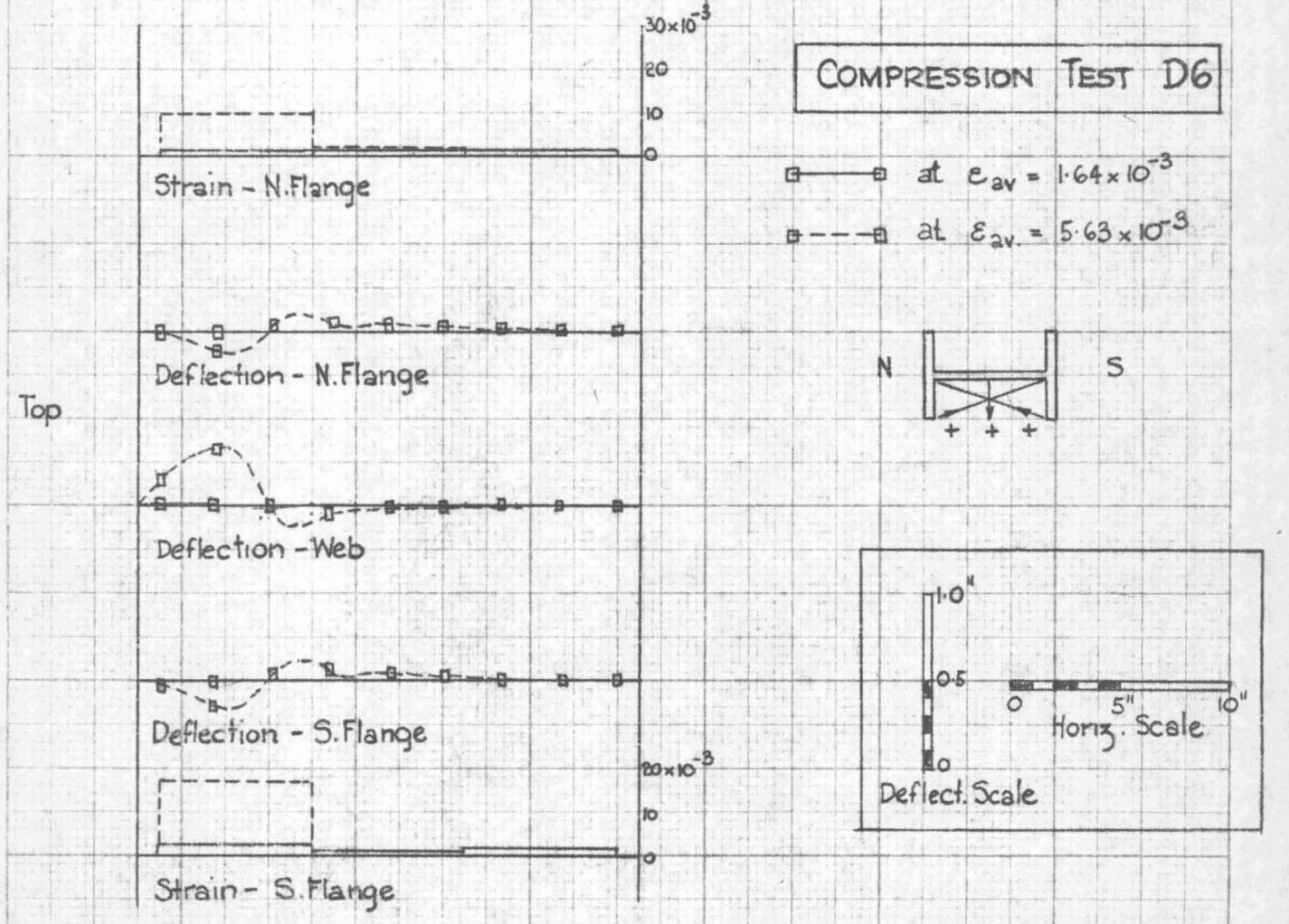

Figure 17. Web and Flange Buckling B6 - D6.

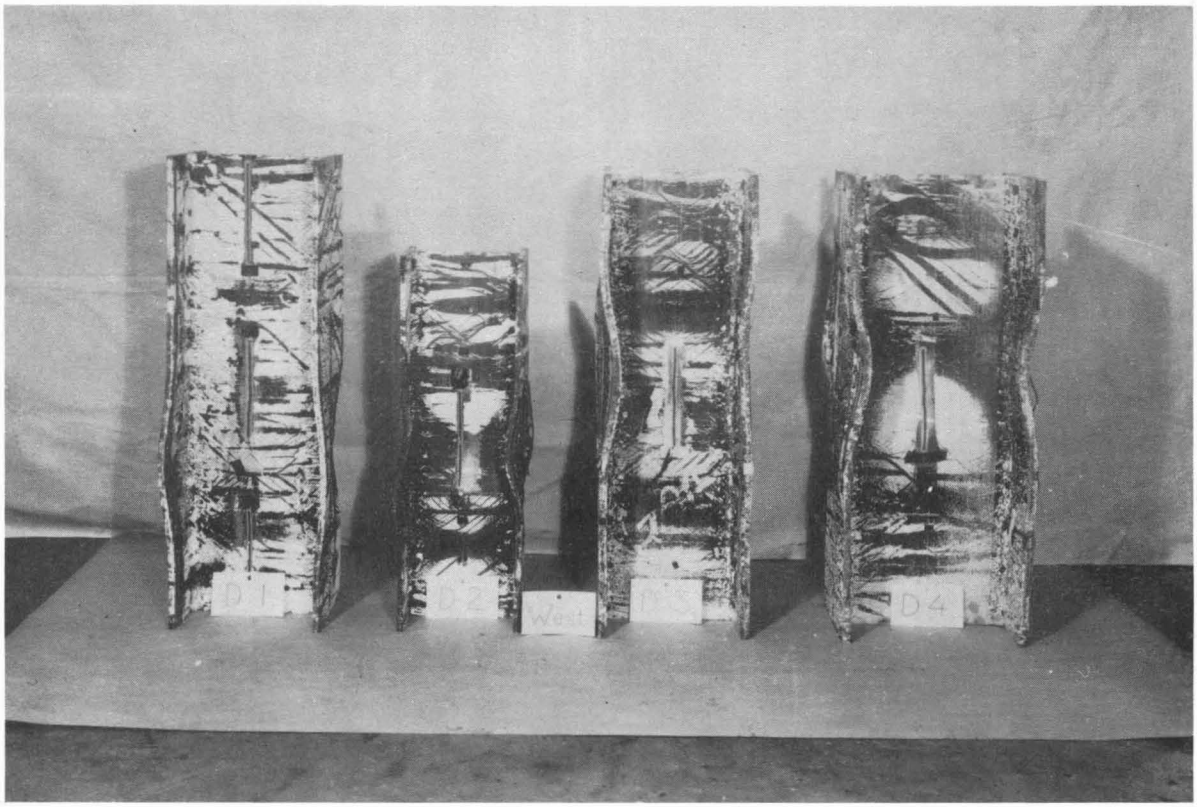

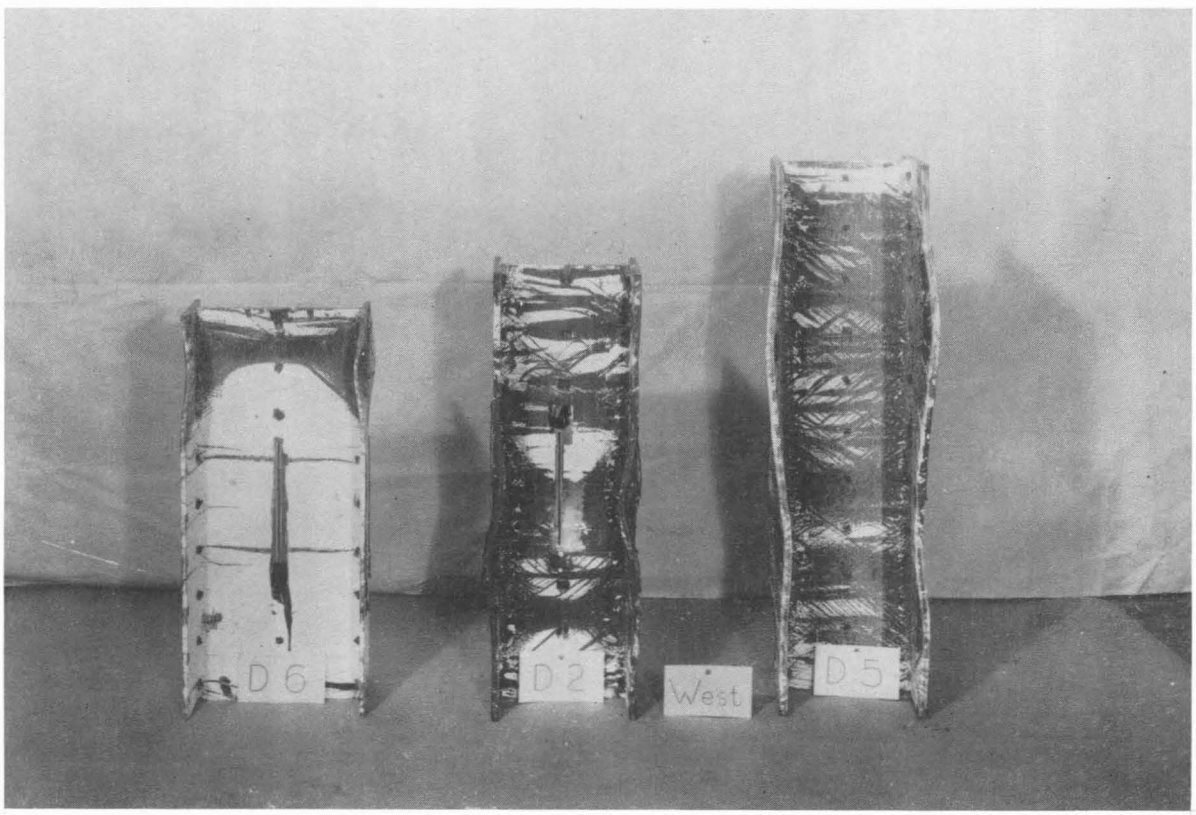

Fig. 18 Compression Specimens After Testing

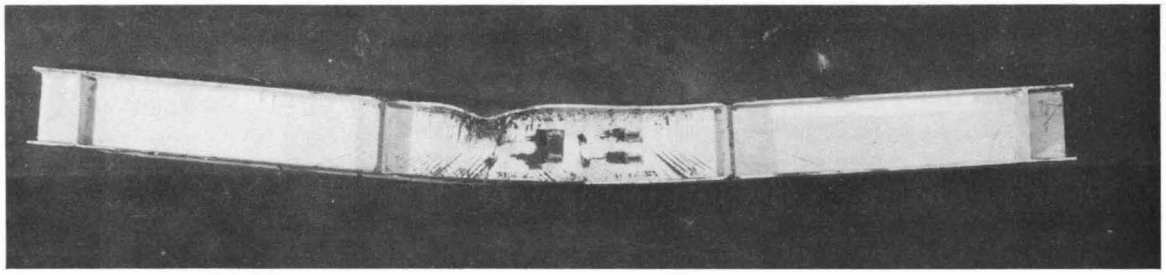

B1

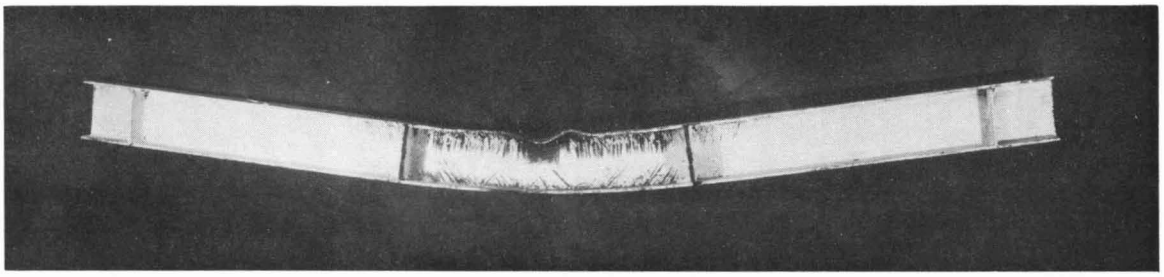

B2

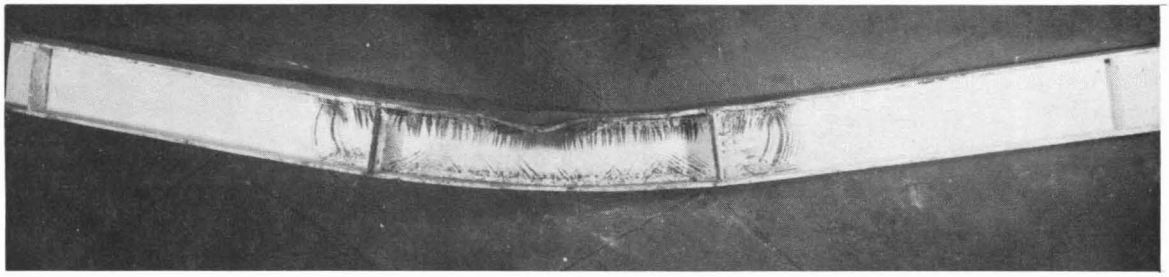

B3

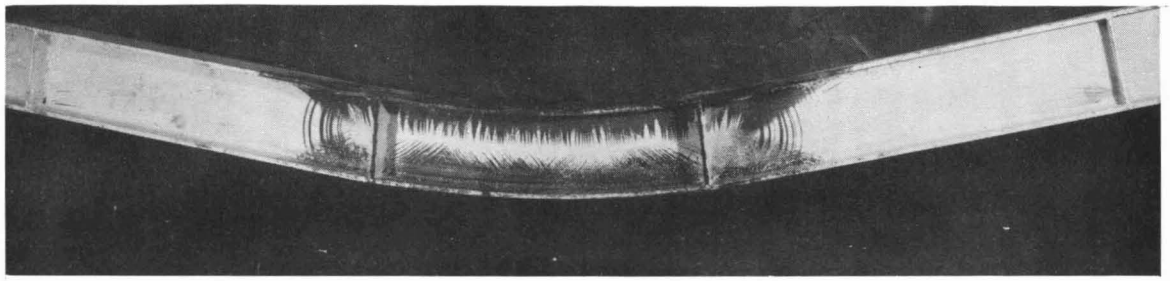

B4

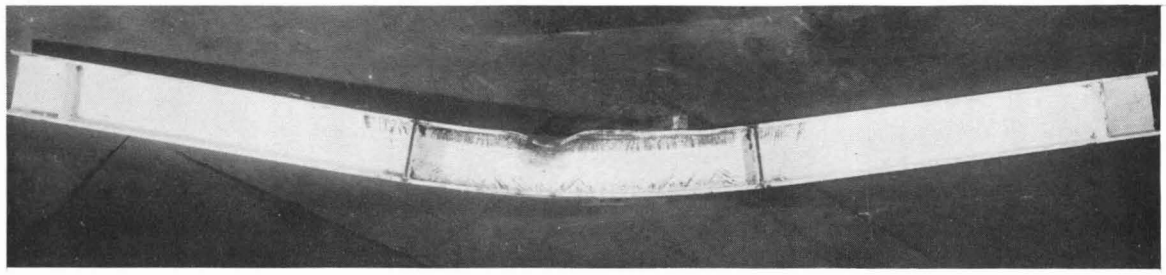

B5

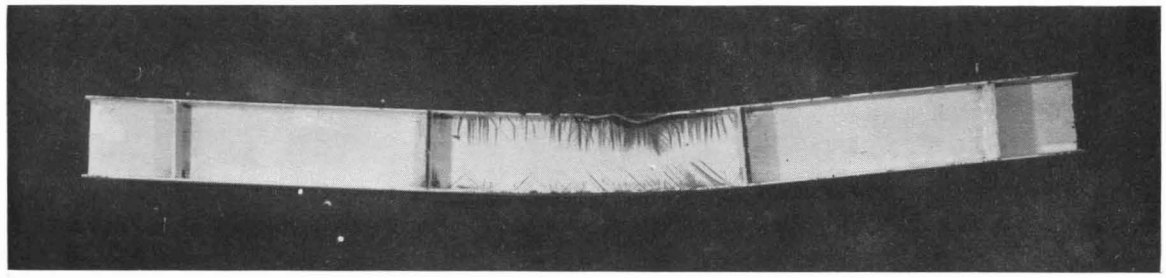

B6

Fig. 19 Side View of Bending Specimens After Testing

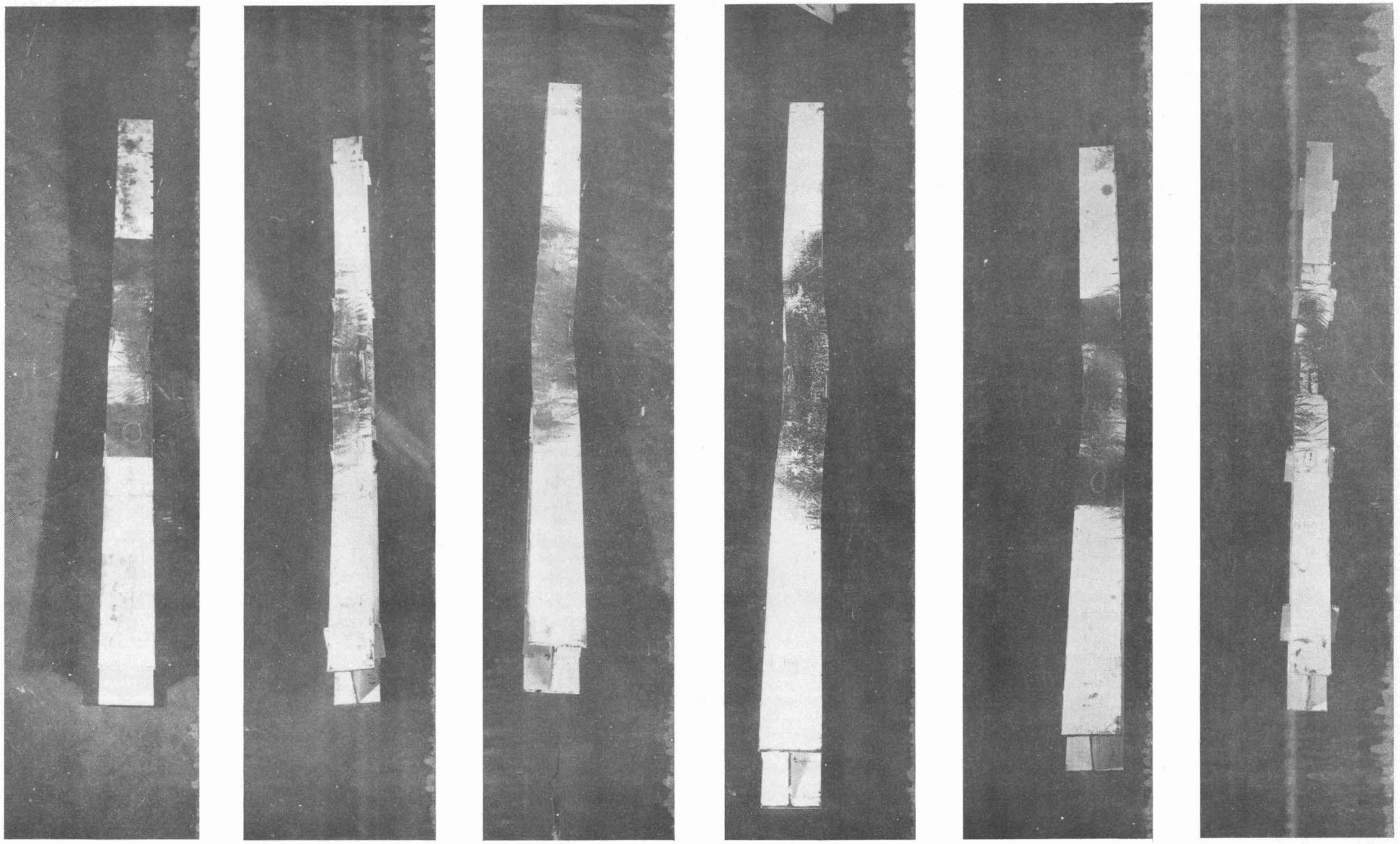

B1 B2 B3 B4 B5 B6

Fig. 20 Top View of Bending Specimens After Testing

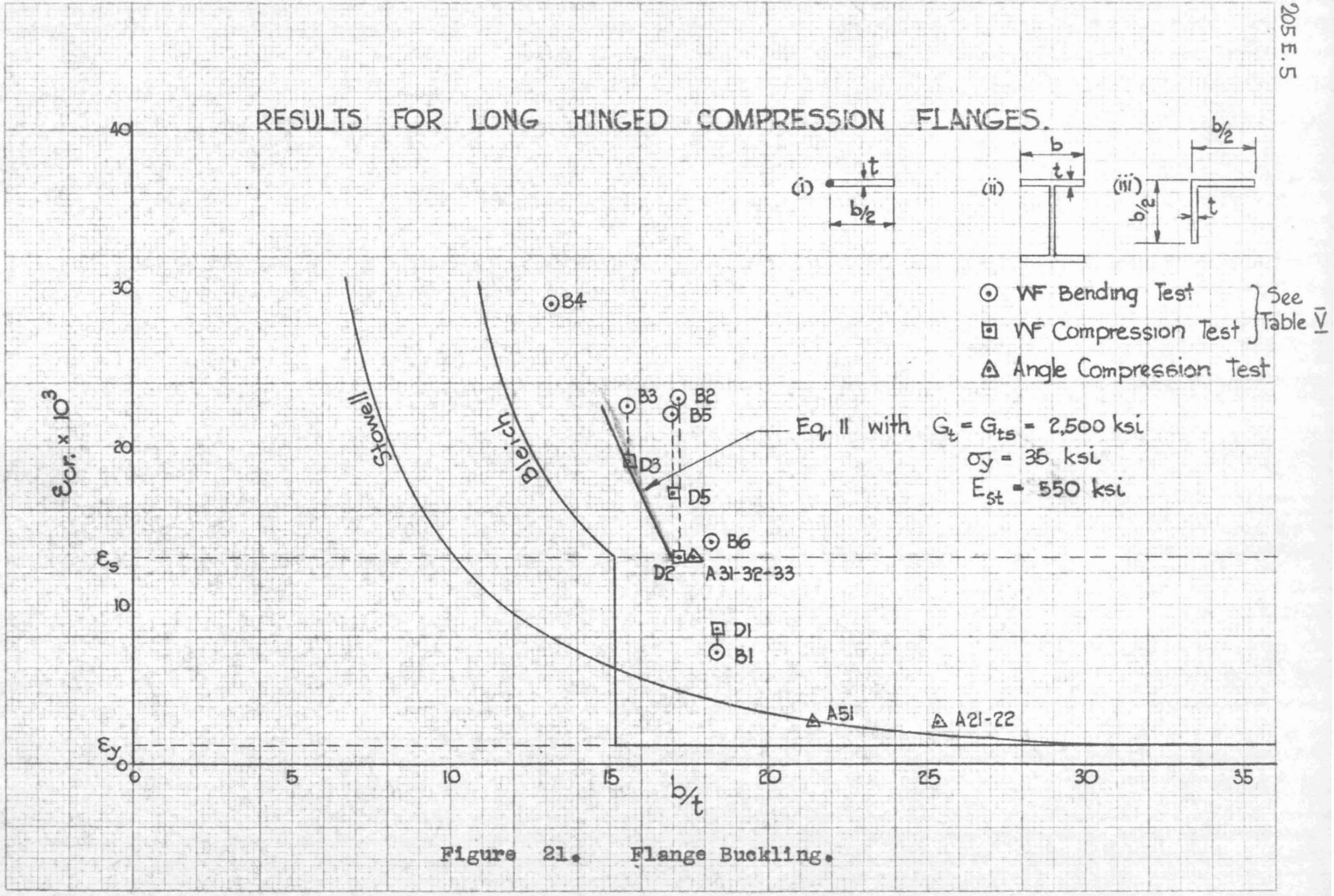

Figure 21. Flange Buckling.

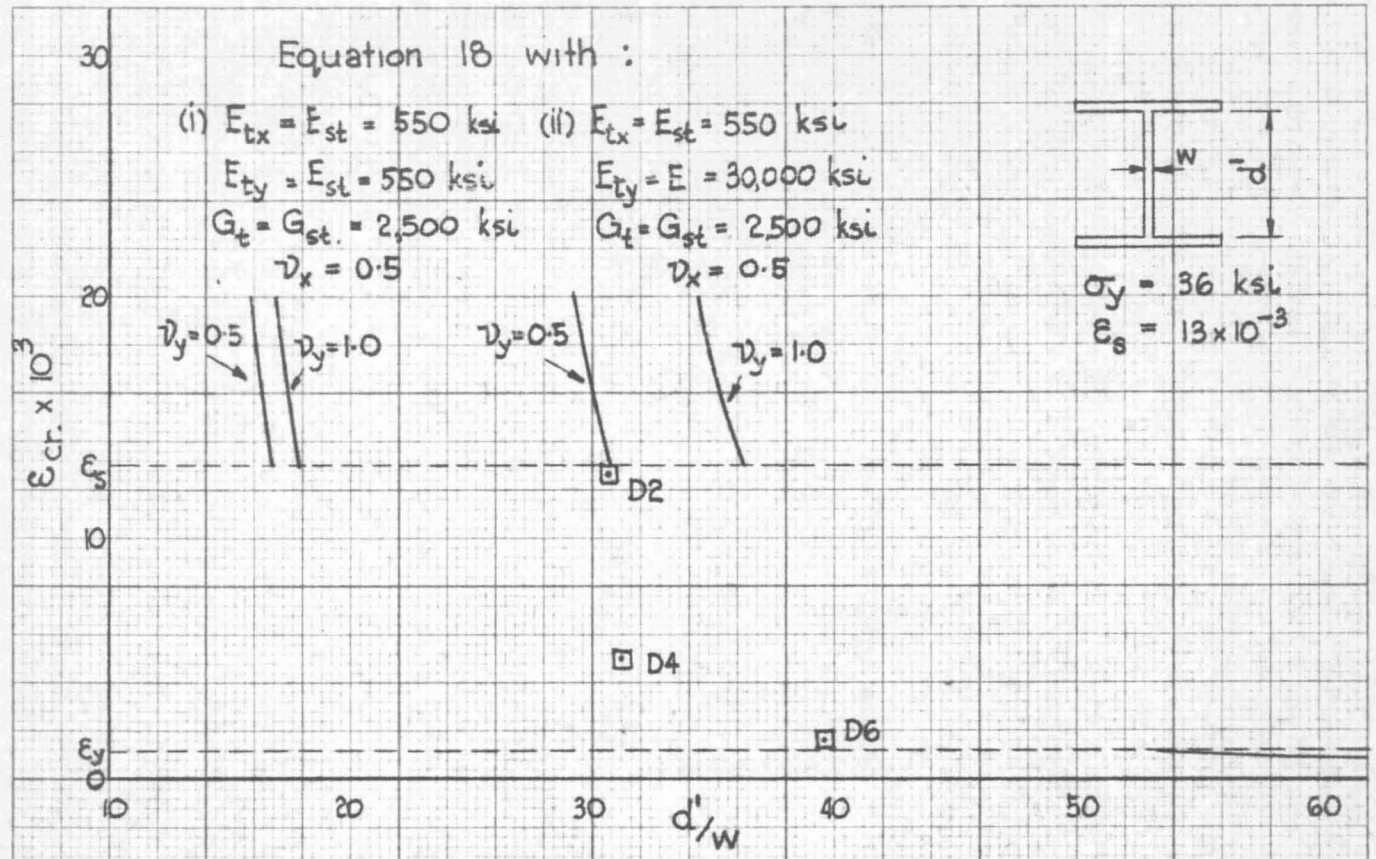

Figure 22. Web Buckling.

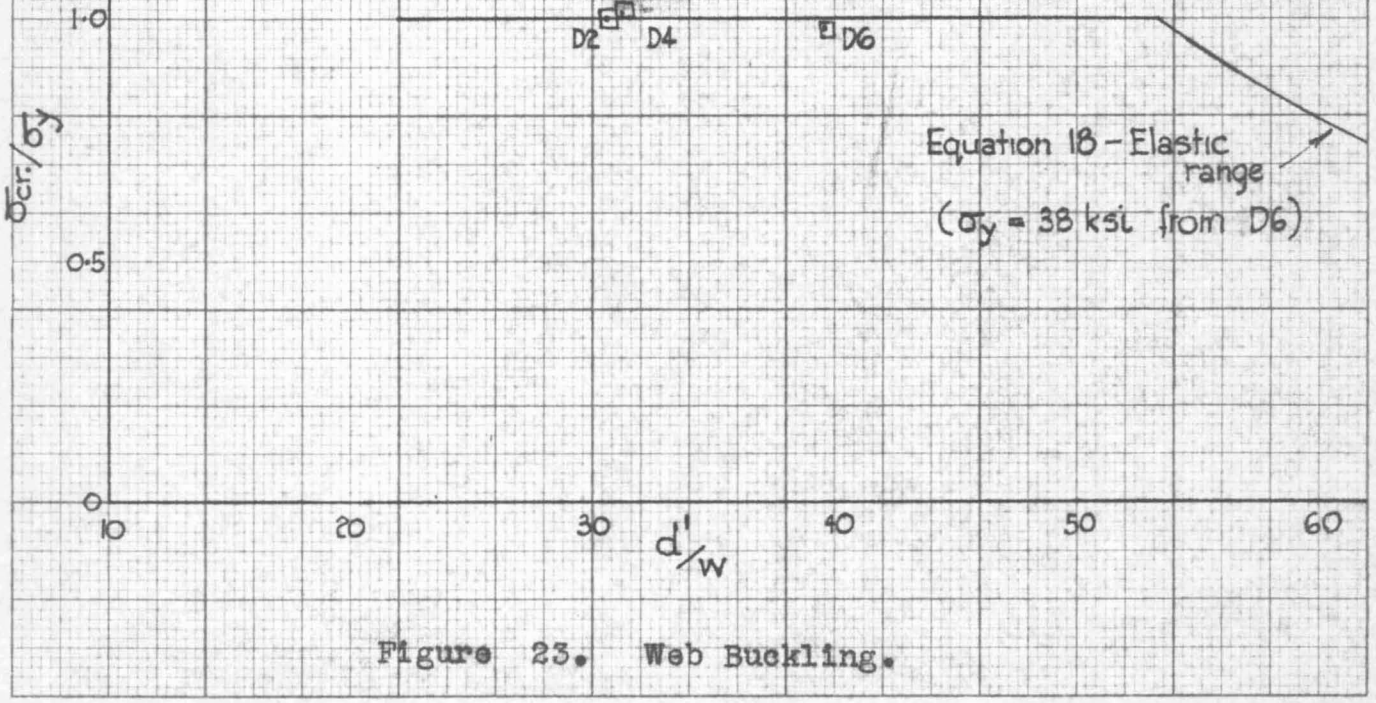

Figure 23. Web Buckling.